

# 44<sup>th</sup> Annual Graduate Student Colloquium



*photo by John Fegyveresi*

Sponsored by Shell  
Hosted by the Department of Geosciences

March 16-17, 2012

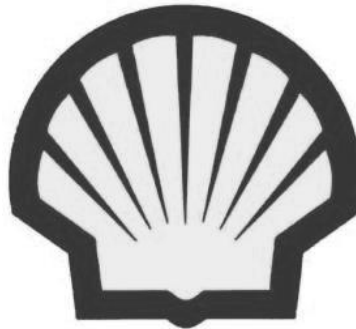


# 44<sup>th</sup> Annual Graduate Student Colloquium

Sponsored by Shell and hosted by the Department of Geosciences  
March 16-17, 2012

The Graduate Student Colloquium is a forum where students present their research or research proposal to faculty, friends, and peers. The Colloquium is hosted by the Department of Geosciences and is open to graduate students involved in geosciences research. The colloquium format stimulates research discussion, allows students to practice for national meetings, and helps students improve their presentation skills. The Colloquium assists both the Department and Penn State in maintaining and strengthening their reputations for giving high quality talks and poster presentations at national and international meetings.

The Graduate Colloquium Committee wishes to thank the students for sharing their work and the faculty for providing constructive feedback. The Committee also wishes to thank the Shell People Services division of Shell Oil Company for their generous financial support, and the Department of Geosciences for hosting this Colloquium.



## Schedule of Events

<i>Event</i>	<i>Date and Time</i>	<i>Location</i>
Poster Viewing	March 16, 6:30-8:30 March 17, 8:30-4:00	EES Atrium
Poster Session 1	March 16, 6:30-7:30	EES Atrium
Poster Session 2	March 16, 7:30-8:30	EES Atrium
Oral Session 1a - Environmental Geochemistry	March 17, 8:30-10:15	114 EES
Oral Session 1b - Geodynamics/Petrology	March 17, 8:30-10:45	116 EES
Break	March 17, 10:30-11:00	
Oral Session 2a - Paleontology	March 17, 11:00-12:15	114 EES
Oral Session 2b - Ice/Hydrology	March 17, 11:00-12:15	116 EES
Lunch	March 17, 12:15-1:15	EES Atrium
Oral Session 3 - Biogeochemistry	March 17, 1:30-2:30	114 EES
Break	March 17, 2:30-3:00	
Oral Session 4a - Astrobiology	March 17, 3:00-4:00	114 EES
Oral Session 4b - Sedimentology/ Stratigraphy	March 17, 3:00-4:00	116 EES
Dinner and Discussion at the Marone's	March 17, 6:30	591 E. Shadow Lane, State College

# Graduate Student Colloquium Committee Members 2012

Jamie Brainard, Chair  
Lauren Milideo, Chair

Ying Cui  
James Deane  
Matthew Gonzales  
Roman Olson  
Kristina Peterson  
Megan Pickard  
April Roberson  
Xuhua Shi  
Anna Wendt

# The Peter Deines Lectureship

The first place award for an oral presentation by a post-comprehensive Ph.D. student is designated the Peter Deines Lectureship for the following academic year.

This award was started in 2004 to represent the tremendous amount of respect and admiration the graduate students in the Department of Geosciences had for Dr. Peter Deines, who that year was stepping down from the position of Graduate Program Chairman. Recipients of the honor are invited to give a departmental colloquium talk during the proceeding academic year.

The department and the world lost a great man and wonderful person when Peter passed away on February 2, 2009. It is with great pride that the Graduate Student Colloquium continues the tradition born in 2004.

## Past Recipients:

2011-2012: Bryan Kaproth

2010-2011: Tim Fischer

2009-2010: Aaron Diefendorf and Bryn Kimball

2008-09: Daniel Hummer

2007-08: Gavin Hayes

2006-07: Christina Lopano

2005-06: Shawn Goldman and Courtney Turich

2004-05: Margaret Benoit

# The Peter Deines Lectureship



Peter Deines (4/02/36 - 2/02/09) earned a Geologen Vordiplom at the Rheinsche Friedrich Wilhelms Universitaet, Bonn, Germany in 1959, an M.S. (1964) and a Ph.D. (1967) in Geochemistry and Mineralogy from Penn State University. Since 1967, and after 2004, as an Emeritus Professor, he was a member of the Geological Science Faculty of the Pennsylvania State University. He earned an international reputation for his geochemical research, teaching, and science administration. Recognition came in teaching awards, election to the University Senate, in which he served for 24 years, and election especially to Treasurer of the International Geochemical Society. In that office, he was so effective that he was awarded a unique Honorary Life Membership for his financial management of the society. He was a principal organizer of that Society's primary international meetings, the famous Goldschmidt Conferences.

With his gift for organization, he also served the Department of Geosciences on most of its committees and he served as its Graduate Program Chairman, while also administering committees for the College of Earth and Mineral Sciences, primarily for Scholarships. Most important was his commitment to the University Academic Senate, in which he served in 28 committee posts, including its Chair for 1990-91; and to the University, on 34 committees and commissions, including University Ombudsman since 2006. He also was elected President of the Faculty-Staff Club. Dr. Deines' research centered on precise explanations of natural variations in stable isotope abundances as means of understanding geologic processes. Results were presented in lectures throughout the world and in over 60 published papers. His illustrated book, "Solved Problems in Geochemistry," was polished by his teaching of eight graduate courses and is available on the web especially for graduate students.

A 40-year member of the Nittany Valley Symphony, Peter will be missed for his finesse with violin and viola.

# Poster Session One

Friday, March 16  
6:30-7:30 pm, EES Atrium

Poster #	Presenter	Advisor	Title
1	Russell Rosenberg	Eric Kirby	Does late Miocene exhumation along the western slope of the Colorado Rockies reflect differential rock uplift?
3	Jennifer Alpern	Chris Marone	Exploring the Physicochemical Processes that Govern Hydraulic Fracture Through Laboratory Experiments
5	Matthew Travis	Pete LaFemina	Strain Partitioning in a Propagating Ridge System: Inter and Intra-Ridge Strain Accumulation in South Iceland
7	Katie Boyle	Andy Nyblade	Ambient seismic noise tomography of the East Africa
9	Yunhui Tan	Terry Engelder	Testing the Gas Plume Hypothesis Using Fracture Distribution above Marcellus
11	Alexander Burpee	Rudy Slingerland	Relationships between sediment caliber and delta shoreline geometry and stratigraphy
13	Tim Murray	Maureen Feineman	Geochemical constraints on the subarc mantle beneath the Andes at 34°S
15	Mike Cleveland	Charles Ammon	Surface-Wave Multiple-Event Relocation and Detection of Earthquakes along the Romanche Fracture Zone

# Does late Miocene exhumation along the western slope of the Colorado Rockies reflect differential rock uplift?

**Russell Rosenberg**

M.S. Student

**Advisor: Eric Kirby**

Andres Aslan, Mesa State College

Karl Karlstrom, University of New Mexico

Matt Heizler, Shari Kelly: New Mexico Institute of Mining and Technology

Rachel Piotraschke, Kevin Furlong: Penn State University

It is increasingly recognized that dynamic effects associated with changes in mantle flow and buoyancy can influence the evolution of surface topography. In the Rocky Mountain province of the western United States, recent seismic deployments reveal intriguing correlations between anomalies in the velocity structure of the upper mantle and regions of high topography. Here, we investigate whether regional correlations between upper-mantle structure and topography are associated with the history of Late Cenozoic fluvial incision and exhumation. Major tributaries of the upper Colorado River, including the Gunnison and Dolores Rivers, which drain high topography in central and western Colorado overlie upper mantle with slow seismic wave velocities; these drainages exhibit relatively steep longitudinal profiles (normalized for differences in drainage area and discharge) and are associated with ~1000-1500 m of incision over the past 10 Ma. In contrast, tributaries of the Green River that drain the western slope in northern Colorado (White, Yampa, and Little Snake Rivers) overlie mantle of progressively higher seismic wave velocities. River profiles in northern Colorado are two to three times less steep along reaches with comparable bedrock lithologies. New  $\text{Ar}^{39}/\text{Ar}^{40}$  ages on ~11 Ma basalt flows capping the Tertiary Brown's Park Formation in northern Colorado indicate that the magnitude of exhumation along these profiles ranges from ~400 – 600 m over this time interval. The correspondence of steep river profiles in regions of greater incision implies that the fluvial systems are dynamically adjusting to an external forcing. New constraints on the exhumation history of the upper Colorado River from apatite fission track ages in boreholes near Rifle, Colorado are best explained by an onset of exhumation at ca. 8-10 Ma. Thus, relative base level fall associated with development of Grand Canyon (ca. 6-5 Ma) does not explain the regional onset of incision along the western slope of the Rockies. Additionally, new cosmogenic burial ages from fan-terrace complexes near Rifle, Colorado show that Colorado River incision occurred at similar rates over both 10 Ma and 2 Ma timescales. Fluvial incision in response to relative base level fall or to changes in regional climate cannot easily explain the history of differential incision along the western slope. Given the correspondence of steep channels, large magnitude incision and regions of low seismic velocity mantle, we suggest that differential rock uplift driven, in part, by differences in the buoyancy and/or convective flow of the mantle beneath western Colorado is the likely driver for Neogene incision.

# **Exploring the Physicochemical Processes that Govern Hydraulic Fracture Through Laboratory Experiments**

**Jennifer Alpern**

M.S. Student

**Advisor: Dr. Chris Marone**

Derek Elsworth, College of Earth and Mineral Sciences, The Pennsylvania State University, University Park, PA 16802

Andrew Belmonte, Department of Mathematics and of Material Sciences & Engineering, The Pennsylvania State University, University Park, PA 16802

Peter Connolly, Chevron Exploration Technology Company, Houston, TX 77002

Hydrocarbon recovery is potentially maximized with an open, complex fracture network of large surface area to volume ratio that penetrates the reservoir. We study the hydraulic rupture of a solid, homogenous cube of Polymethyl methacrylate (PMMA) containing model boreholes as an analog to hydraulic fracturing with various fracture-driving fluids. The transparency of PMMA allows for the visualization of fracture propagation using high-speed video. The cubes are constrained by prescribed triaxial far-field stresses with the borehole-parallel stress set to zero. The cube is ruptured by overpressuring the borehole at controlled rates with fluids present as both liquids and gases pre- and syn- failure. We measure the fracture breakdown pressure, rates of fracture propagation and the physical characteristics of the resulting fractures and how they vary between fluid types (Figure 1). Further research extends these experimental methods to bluestone and granite, with additional tests that determine the permeability of these materials and its effect on creating a complex fracture network.

# Strain Partitioning in a Propagating Ridge System: Inter and Intra-Ridge Strain Accumulation in South Iceland

**Matthew Travis**

M.S. Student

**Advisor: P. LaFemina**

H. Geirsson, Pennsylvania State University, USA

E. Sturkell, University of Gothenburg, Sweden

F. Sigmundsson, University of Iceland, Iceland

T. Arnadóttir, University of Iceland, Iceland

S. Hreinsdóttir, University of Iceland, Iceland

The Mid-Atlantic Ridge, the slow spreading (~20 mm/yr) mid-ocean ridge boundary between the North American and Eurasian plates, is exposed subaerially in Iceland as the result of ridge-hotspot interaction. Plate spreading in Iceland is accommodated along neovolcanic zones comprised of central volcanoes and their fissure swarms. In south Iceland plate motion is partitioned between the Western Volcanic Zone (WVZ) and Eastern Volcanic Zone (EVZ). The two systems are connected by the south Iceland seismic zone (SISZ), a left-lateral transform zone. Plate motion across both systems has been accommodated by repeated rifting events and fissure eruptions. In this study we investigate two main questions: 1) What is the magnitude and spatial distribution of strain accumulation in south Iceland, and 2) Is strain accumulation localized to one fissure swarm, or are multiple systems active? We use horizontal velocities based on continuous and episodic GPS measurements from 2000-2010 to calculate strain rates and constrain block models that investigate relative block motion and coupling along block-bounding faults. Our strain rate calculations indicate the greatest dilational strain is currently being accumulated on the western edge of the EVZ. This is centered near Hekla volcano in the south, and west of the Veidivotn and Vatnaöldur fissure swarms, both of which have had large volume historical fissure eruptions, further north. Further dilation is seen at the southern tip of the Lakagigar fissure swarm and south of Torfajökull volcano. Results of block modeling indicate no strain accumulation in the northern WVZ and that strain accumulation in the EVZ is not localized to a single fissure swarm, but rather distributed across the entire EVZ. Our models also predict locking depths of < 2.5 km in the WVZ and 20-30 km in the EVZ. We found locking depths in the SISZ to be 5-15 km, which are consistent with past estimates.

# **Ambient seismic noise tomography of the East Africa**

**Katie Boyle**  
M.S. Student

**Advisor: Andy Nyblade**

Ambient seismic noise recorded on approximately 75 stations in East Africa is being used to study the shear wave velocity of the crust. Cross correlation of the noise reveals short-period Rayleigh waves that are well-recorded on many stations. Group velocities of the Rayleigh waves were measured, with the best results occurring between 5 and 25 second periods. Group velocities measured from earthquakes are being used to supplement the data set and fill in gaps in raypath coverage. Group velocities for each period are obtained by inverting the ensemble of measurements. Low wave speed anomalies that correlate with sedimentary basins can be seen at 5 and 15s periods.

# Testing the Gas Plume Hypothesis Using Fracture Distribution above Marcellus

**Yunhui Tan**

Ph.D. Student, Pre-comps

Petroleum related

**Advisor: Terry Engelder**

Tom Johnston, School of Earth & Ocean Sciences, University of Southampton, Southampton, United Kingdom

Terry Engelder, Department of Geosciences, Pennsylvania State University, State College, PA, United States

Joints in the Middle and Upper Devonian formations of the Appalachian Basin, the Catskill Delta Complex, are common, particularly in the silt- and sandstone layers. The planar surface and cyclic plumose morphology indicate these joints are gas driven. Generally two sets of joints can be seen: J1 and J2. The strike of J1 joints range from  $060^{\circ}$  to  $085^{\circ}$ , while those of J2 joints range from  $320^{\circ}$  to  $010^{\circ}$ . J1 is present in organic rich shales and rapidly disappears above these source rocks, while J2 appears in coarser clastic rocks of the delta complex as much as 2000 m above the Marcellus. This pattern was discovered through mapping 281 outcrops in Northeastern Pennsylvania and Central New York. The fraction of outcrops with joints present decreases up section above either Marcellus Shale or the Genesee/Burket when present. Gas-driven joints are present in 100% of the Brallier Formation outcrops, 76% of the Lock Haven Formation, 58.2% of the Catskill Formation, 20% of the Huntley Mountain Formation and 0% of the Monongahela Formation outcrops. Joint density also decreases with vertical height above the source rocks when compared on an outcrop by outcrop basis.

To explain the distribution of gas-driven J2 joints, we propose a gas plume model. Gas plumes reflect pervasive leakage above source rock due to buoyancy of overpressured methane gas. A gas column is more likely to overcome the least horizontal rock stress at the top of the column. The core of the gas plume is taken to be the volume of rock just above the source rock where joint density is highest. Further up in the section where methane pressure dissipates, the density of joints decreases in a logarithmic trend away from the gas plume core. Some areas above source rocks are more densely jointed than expected and these are interpreted as gas chimneys.

Most joints in the Catskill Delta Complex are not mineralized, further evidence for pervasive methane. The joints of the gas plume may well have served as a conduit for methane migration from the deep black shales to charge shallow sand layers during late Palaeozoic maturation of the Devonian source rocks.

# Relationships between sediment caliber and delta shoreline geometry and stratigraphy

**Alexander P. Burpee**

M.S. Student, Petroleum related

**Advisor: Dr. Rudy Slingerland**

Dr. Doug Edmonds, Boston College

Recent morphodynamic modeling of non-uniform turbulent transport and deposition of sediment in a standing body of water devoid of tides and waves shows that sediment caliber plays a major role in determining the shapes, cumulative number of distributaries, and wetland areas of river-dominated deltas. In this study we introduce metrics for quantifying delta shoreline rugosity and foreset dip (clinoform) variability, and explore their variation with sediment caliber. Delta shoreline rugosity is calculated using the isoperimetric quotient,  $IP = 4 \pi A / P^2$ , where a circle has a value of one. Clinoform complexity is calculated using the uniformity test in circular statistics wherein clinoform dip direction uniformity is the sum of the deviations of dip azimuths from a theoretical uniform distribution. Analysis of fifteen simulated deltas shows that IP increases from 0.1 to 0.5 as the normalized shear stress for re-erosion of cohesive sediment,  $\tau_n$ , increases from 0.65 to 1. Clinoform dip azimuth uniformity decreases from 300 to 130 with increasing  $\tau_n$ . Preliminary analysis of data from outcrops of the Cretaceous Ferron Delta is consistent with these trends. These results imply that changes in sediment caliber delivered to a deltaic coastal system will profoundly change its wetland area, bathymetric hypsometry, ecological function, and interior stratigraphy.

# Geochemical constraints on the subarc mantle beneath the Andes at 34°S

**Tim Murray**

M. S. Student

**Advisor: Maureen Feineman**

Other authors: Maureen Feineman, Penn State University

Arc magmas from the Northern Southern Volcanic Zone (NSVZ) of the Andes are characterized by distinct geochemical signatures that have been the center of much debate. These signatures, including  $^{87}\text{Sr}/^{86}\text{Sr} > \sim 0.7045$ ,  $\text{Sr}/\text{Y} > 35$ , and  $\text{La}/\text{Yb} > 12$ , suggest incorporation of a crustal component during magma genesis. One hypothesis for the crustal component of the geochemical signatures proposes a period of magma stalling and mixing at the base of the exceptionally thick (>50 km) crust beneath the arc in this region [1]. Others argue for contamination of the mantle source by subducted crustal material as the result of subduction erosion [2]. Because both involve assimilation of crustal material at similar pressures and temperatures, it is difficult to discern between the two on the basis of geochemical signatures of the arc magmas. Furthermore, the arc magmas in the NSVZ lack basaltic lavas, increasing the difficulty of gauging the nature of the subarc mantle. However, The Quaternary Payenia volcanic province, situated about 50 km from the arc axis, does contain primitive basalts that provide constraints on the composition of the mantle at this latitude[3]. We have sampled seven olivine basalt lava flows, tephra rings, maars, and cinder cones from this province between 34°15' and 34°45' S. The Sr isotopic composition of these primitive basalts is  $^{87}\text{Sr}/^{86}\text{Sr} = 0.7040 \pm 0.0004$  (2s), which is statistically different from the basaltic andesites and andesites located on the arc front at the same latitude, which have  $^{87}\text{Sr}/^{86}\text{Sr} = 0.7050 \pm 0.0004$  (2s). The rear-arc basalt values closely match those found on the volcanic front further south, which are generally not considered to show evidence of similar crustal contamination. A model of magma stalling and mixing at the base of thick crust beneath the arc would allow for the presence of a “normal” (*not* crustally contaminated) mantle composition. This would explain the presence of low  $^{87}\text{Sr}/^{86}\text{Sr}$  ratios in the rear-arc basalts compared to the arc andesites in the NSVZ, since the crust is significantly thinner beneath the rear-arc and volcanic features appear along tectonically controlled NW-SE lineaments, allowing the unadulterated mantle composition to be expressed. Conversely, if subduction erosion is the driving force for the signatures we see in the arc magmas of the NSVZ, then the subarc mantle must be decoupled from the mantle feeding the Payenia volcanic province.

[1] Hildreth and Moorbath (1988) *CMP* **98**, 455-489.

[2] Kay et al. (2005) *GSA Bull.* **117**, 67-88.

[3] Ramos and Folguera (2011) *JVGR* **201**, 53-64.

# **Surface-Wave Multiple-Event Relocation and Detection of Earthquakes along the Romanche Fracture Zone**

**Michael Cleveland**

Ph.D. Student, Pre-comps

**Advisor: Charles Ammon**

Tom VanDeMark, AFTAC

The Romanche Transform system, located along the equatorial Mid-Atlantic Ridge, is approximately 900 km in length and separates plates moving with a relative plate speed of three cm/yr. We use cross-correlation of globally recorded Rayleigh waves to estimate precise relative epicentroids of moderate-size earthquakes along the Romanche Fracture Zone system. The Romanche transform has an even distribution of large events along its entire length that provide a good base of events with excellent signal-to-noise observations. Two distinct moderate-magnitude event clusters occur along the eastern half of the transform and the region between the clusters hosted a large event in the last decade. Based on initial results (Van DeMark, 2006), unlike those of shorter transform systems, the events along the Romanche do not follow narrow features, the event clusters seem to spread perpendicular as well as laterally to the transform trend. These patterns are consistent with parallel, en echelon and/or braided fault systems, which have been previously observed on the Romanche through the use of side scanning sonar (Parson and Searle, 1986). We also explore the character and potential of seismic body waves to extend the method to help improve relative event depth estimates. Relying on a good base of larger and moderate-magnitude seismicity, we attempt to extend the analysis by processing continuous data streams through processes measuring waveform similarity (e.g. cross-correlation) in an attempt to detect smaller events using a subset of nearest seismic stations.

# Poster Session Two

Friday, March 16  
7:30-8:30 pm, EES Atrium

Poster #	Presenter	Advisor	Title
2	Claire Mondro	Don Fisher	Deformation history of the Taiwan orogenic belt, as measured by syntectonic pressure shadows
4	Katelyn Olcott	Damien Saffer	Constraints on in situ stresses in the Nankai Trough, offshore SW Japan from borehole breakouts and laboratory measurements of rock strength
6	Alysa Young	Andy Nyblade	The Crustal Structure of Tanzanian Coastal Basins using P-wave Receiver Functions
8	John Fegyveresi	Richard Alley	Seasonal influences on firn layering and bubble trapping, WAIS Divide, West Antarctica
10	James Deane	Maureen Feineman	Equilibrium Partitioning of Li between Olivine and Clinopyroxene at Mantle Conditions
12	Piyali Chanda	Matt Fantle	Magnesium and strontium concentrations in pore-fluids of deep sea sediment cores : Importance in determination of paleo-seawater composition
14	Gabriel Mulibo	Maureen Feineman	Mantle Structure beneath East Africa and Zambia from Body wave Tomography
16	Amanda Martino	Christopher House	Microbial community composition of marine subsurface samples from equatorial Pacific and Peru margin locations after multiple whole genome amplification methods

# Deformation history of the Taiwan orogenic belt, as measured by syntectonic pressure shadows

**Claire Mondro**

M.S. Student

**Advisor: Don Fisher**

The island of Taiwan is formed by collision of the Asian continental margin and the Luzon volcanic arc. The tectonic history of the island illustrates a type-example of arc-continent collision zones. Accepted models of the orogenic system describe it as a critically tapered, asymmetric, doubly-vergent wedge (Fuller et al., 2006). Accreted material enters the orogen on the west side and advects to the eastern surface along hyperbolic paths, so the longest paths are recorded by rocks east of the divide. Previously observed changes in cleavage plane orientation across the Central Range support the hypothesis that the wedge is doubly-vergent (Fisher et al., 2007). Finite strain indicators also display large differences in orientation of max stretch west to east across Taiwan from down dip extension in the west to along strike extension in the east, suggesting variations in stretch direction that are tied to mountain belt geometry. My in-progress research measures the incremental strain history of the deformation from curved pressure shadows within Eocene slates from the eastern edge of the Central Range, which have traveled a complete advection path through the system. An incremental strain history will show changing stress orientation at chronological points along a 3-D advection path through the critical wedge. My hypothesis is that samples in eastern Taiwan will record systematic temporal variations from down-dip extension to along-strike extension that correspond to changing extension directions from west to east.

Fisher, D., S. Willett, Y. En-Chao, and M.B. Clark, 2007. Cleavage fronts and fans as reflections of orogen stress and kinematics in Taiwan. *Geology* 35(1), 65-68, doi:10.1130/G22850A.1.

Fuller, C.W., S.D. Willett, D. Fisher, and C.Y. Lu, 2006. A thermomechanical wedge model of Taiwan constrained by fission-track thermochronometry. *Tectonophysics* 425, 1-24.

# Constraints on in situ stresses in the Nankai Trough, offshore SW Japan from borehole breakouts and laboratory measurements of rock strength

**Katelyn Allison Huffman Olcott**

Ph.D. Student, Pre-comps

**Advisor: Demian Saffer**

Hiroko Kitajima: Dept. of Geosciences and Center for Geomechanics, Geofluids, and Geohazards, The Pennsylvania State University

Demian Saffer: Dept. of Geosciences and Center for Geomechanics, Geofluids, and Geohazards, The Pennsylvania State University

Quantifying in situ stress orientation and magnitude in active tectonic settings is important toward understanding mechanics and absolute strength of faults, yet direct measurements of these quantities are scarce. Stress magnitude estimates can be obtained by combining constraints from observation of compressional wellbore failures (BO) and the limits of frictional sliding on optimally oriented faults. We use BO width documented by Ocean Drilling Program (ODP) drilling in the accretionary wedge of the Nankai subduction zone offshore SW Japan to constrain magnitudes of maximum and minimum horizontal stresses ( $S_{Hmax}$  and  $S_{Hmin}$ ). During ODP Legs 131 and 196, drilling and coring at Site 808, located ~3 km landward of the trench, penetrated the accretionary wedge, plate boundary décollement, and underthrusting sediments. Logging while drilling resistivity-at-the-bit (LWD) images are available to 825 mbsf and document BO in the lowermost accretionary wedge. Stress magnitudes are estimated from (1) BO width, which depends on rock mechanical properties such as unconfined compressive strength (UCS), Poisson's ratio ( $n$ ), and internal friction coefficient ( $\mu_i$ ), formation pore pressure ( $P_f$ ), and annular fluid pressures, and (2) Coulomb failure on pre-existing faults which depends on coefficient of sliding friction ( $\mu$ ) and  $P_f$ . We calculate a range of UCS from empirically derived relationships between p-wave velocity ( $V_p$ ) and UCS. We assume values of  $\mu = 0.4$ ,  $\mu_i = 0.4$ , and  $n = 0.45$  and consider a range of  $P_f$  values, from hydrostatic to ~75% of lithostatic. Resulting stress magnitudes are most sensitive to UCS and less sensitive to the choice of  $\mu_i$  or  $n$ .  $P_f$  affects criteria for generating BO and for slip on existing faults, and thus has a large effect on stress estimates. For the case of hydrostatic  $P_f$ ,  $S_{Hmax}$  (from seafloor) increases from 5.7-9.1 MPa at 364 mbsf, to 11.7-16.0 MPa at 815 mbsf, and is consistent with a thrust or strike-slip faulting regime. For certain depths in overpressured conditions, values of  $S_{Hmax}$  computed from BO widths are not consistent with limits defined by the failure criteria for slip on existing faults, suggesting that UCS is higher than we estimate, or that  $P_f$  cannot be 75% of lithostatic throughout the section. Values of  $S_{Hmax}$  are not consistent with slip on active thrust faults throughout the accretionary wedge. This could be explained if stress varies through the seismic cycle, such that  $S_{Hmax}$  in the outer accretionary wedge is transiently increased following large earthquakes to allow active thrusting. Ongoing triaxial tests on core samples will provide direct measurements of UCS to better constrain stress magnitudes.

# **The Crustal Structure of Tanzanian Coastal Basins using P-wave Receiver Functions**

**Alysa Young**  
M.S. Student

**Advisor: Andrew Nyblade**

The structure of Jurassic to Neogene coastal basins along the Tanzania passive margin and crustal thickness beneath them are being investigated in this study using P-wave receiver functions. Seismic data recorded by eight stations deployed from February 2010 through July 2011 provide the primary dataset. Receiver functions have been computed using ~460 teleseismic events, of which a maximum of 20 were used for each station. The resulting waveforms, consisting of several Ps arrivals in the first 5s, indicate complicated basin structure. To estimate crustal thickness, the h-k stacking method was used for each station. Well-resolved results from one station yield crustal thickness of approximately 38km, with an average  $V_p/V_s$  of 1.67. This station provides reliable results using this method because the station resides on primarily basement rocks and, therefore, has a clear Moho signal. Sediment-filled basins below the other stations produce a ringing effect that masks the Moho's arrival and need to be interpreted using other methods. To roughly estimate basin thickness, the Ps arrival times from the sediment-rock interface and its multiples can be combined with assumed  $V_p/V_s$  ratios for shales and sandstone. Basin thicknesses of between 2 and 6km were obtained. Currently, synthetics and joint inversions are being computed as another approach in determining basin thickness. Preliminary results show basin thicknesses of a few kilometers and uncertain Moho depths. Accurately modeling the upper crust will allow a reliable model of the lower crust. Future work will consist of joint inversions that incorporate more region-appropriate dispersion curves to further constrain Moho depths. Results from each approach will, together, provide the best estimate of basin and crustal structure for this region.

# **Seasonal influences on firn layering and bubble trapping, WAIS Divide, West Antarctica**

**John Fegyveresi**

Ph.D. Student, Pre-comps

**Advisor: Richard B. Alley**

Deposition and near-surface diagenesis on ice sheets create layering in firn that may influence the climatic record and associated proxy data preserved in ice cores, including the number-density and volume of trapped bubbles. Diurnal and seasonal variations, as well as the timing of accumulation in polar regions, affects the near-surface firn through changes in the exposure to various meteorological, atmospheric, and turbulent fluxes. These changes can result in greater surface metamorphism, evaporation, sublimation, convection in the snow pack, surface crusting, and more pronounced grain growth. At sites with relatively high accumulation rates and numerous individual depositional events per year, such as WAIS Divide, these near-surface processes can result in highly layered, irregularly-stratified firn with numerous internal features and high density contrast. If preserved at depth, this high degree of layering may affect bubble trapping at pore close-off and the resulting ice-core proxy data. Here we have been investigating recently obtained data from the WDC06A ice core, in order to discern evidence of these possible seasonal biases.

Real-time snowpit, surface, meteorological and net-solar energy data from four concurrent WAIS Divide field seasons have been analyzed in order to better quantify the conditions and net-surface energy flux surrounding near-surface metamorphism. Distinct and pronounced surface crusts, or “glazes”, are observed frequently at the site. These noteworthy features, and the processes which lead to their formation, are not yet well understood. Observations indicate that these glazes and their associated surface cracks and polygons are more likely to form during relative low-wind, low-humidity, high-temperature episodes. During each documented case, these episodes were brought about by clear-sky days with maximum diurnal variability of incoming solar energy. Furthermore, distinct hoar frost growth was observed on crusts that were exposed to multiple clear-sky days. Observations in the ice core suggest that the pronounced surface crusts also form in wintertime, but are more common in summer. Measurements to assess possible effects of these features on bubble number-density, total trapped air, and grain size and orientation in the core are ongoing.

# Equilibrium Partitioning of Li between Olivine and Clinopyroxene at Mantle Conditions

**James A. Deane Jr.**

M.S. Student

**Advisor: Maureen Feineman**

Jessica Yakob, Pennsylvania State University

David H. Eggler, Pennsylvania State University

Sarah Penniston-Dorland, University of Maryland, College Park

The lithium isotope system holds great allure as a tracer of recycled subducted materials in the Earth's interior, owing to the striking isotopic contrast between lithium at the Earth's surface and that in the mantle, combined with the presence of Li at measurable quantities in mantle minerals. Unfortunately, mantle xenolith data compiled from samples worldwide have revealed that lithium elemental and isotopic distribution between olivine and clinopyroxene is highly variable. At high temperatures, the isotopic fractionation factor  $\alpha_{ol/cpx} [=({}^7\text{Li}/{}^6\text{Li})_{ol}/({}^7\text{Li}/{}^6\text{Li})_{cpx}]$  is expected to approach 1, and experimental constraints on equilibrium partitioning show that the partition coefficient ( $D_{ol/cpx}^{Li}$ ) is between 1.5-2. Many xenolith samples exhibit equilibrium behavior with respect to both isotopic fractionation and equilibrium partitioning, but some samples do not. Xenoliths with apparent  $D_{ol/cpx}^{Li} < 1$  trend toward isotopically lighter Li in clinopyroxene relative to olivine, with  $\Delta^7\text{Li}_{ol-cpx} [= \delta^7\text{Li}_{ol} - \delta^7\text{Li}_{cpx}]$  ranging from 3 - 25‰. A physical process explaining this extreme isotopic fractionation between co-existing mantle phases has yet to be satisfactorily demonstrated. One proposed hypothesis to explain the apparent Li isotopic disequilibrium in mantle xenoliths is that upon exhumation, closed system redistribution of Li between mantle minerals occurs as a function of cooling, meaning the partition coefficient is temperature dependent. Richter et al. (2003) have shown potential for considerable kinetic isotopic fractionation of Li during diffusion. Thus if Li is redistributed during cooling, kinetically driven isotopic fractionation might be "locked in" to the mantle minerals upon reaching closure conditions. We have conducted a series of piston cylinder experiments at 1.5 GPa and 700-1100 °C, the results of which show that  $D_{ol/cpx}^{Li}$  is  $2.0 \pm 0.2$  regardless of temperature over this range. It seems that a new explanation is needed to explain the Li signature in mantle xenoliths. Mantle olivine contains some amount of iron (~10% FeO\*), and the ambient  $fO_2$  controls the relative amount of  $\text{Fe}^{+2}/\text{Fe}^{+3}$ . Variation in the amount of  $\text{Fe}^{+3}$  could potentially influence the incorporation of  $\text{Li}^+$  into the octahedral site of olivine by providing a charge-balancing mechanism. This could allow for a redistribution and isotopic fractionation of Li in response to changing  $fO_2$ . Experiments at 900°C and 1.5 GPa with solid state  $fO_2$  buffers of Re-ReO, Ni-NiO, and Mo-MoO are currently underway to determine whether oxygen fugacity plays a role in controlling Li partitioning.

[1] Richter et al. (2003) *Geochimica et Cosmochimica Acta* 67, 20, 3905–3923.

# **Magnesium and strontium concentrations in pore-fluids of deep sea sediment cores : Importance in determination of paleo-seawater composition**

**PIYALI CHANDA**

Ph.D. Student, Pre-comps

**Advisor: MATTHEW S. FANTLE**

The trace metal compositions of marine carbonate minerals precipitated from the seawater are being widely used as proxies for the studies of paleoclimate, paleoceanography and surface processes responsible for elemental cycles. Mg and Sr particularly gain interest in Paleothermometry as Mg/Ca ratio and Sr/Ca ratio in biogenic carbonates like foraminiferal tests have temperature sensitivity and hence can be used to determine Paleotemperature. The main assumption for this paleotemperature determination is the temperature being the guiding factor that influences the incorporation of Mg in the calcitic foraminiferal tests. But the other important factors that can also govern the Mg/Ca ratio in foraminiferal test are ambient composition of seawater, partition coefficient of Mg and Sr between the seawater and biogenic calcite and the post-depositional diagenetic alteration of the calcite. If the concentrations of the elements in the seawater has changed over the geologic time this change can also affect the incorporation of that metal in calcite tests. One way to investigate the past changes in Mg and Sr concentration in seawater is to study the pore fluid co-existed with the solid sediment in the deep sea cores because this pore fluid is the seawater trapped into the interstitial spaces of the sediments during sedimentation. Now if the rate of sedimentation is high, the sediment and porefluid get buried quickly below the surface and get isolated from the overlying seawater. Therefore, in the region of high sedimentation rate the porefluid will get better chances to preserve the ambient seawater composition because the chances of diffusion from the top seawater will be lesser in that case.

If we consider that there is exchange reaction of Mg between porefluid and biogenic calcite, then the porefluid composition will shift from its original composition to some extent. In this study, the Mg, Ca and Sr concentration of the porefluids from numerous ODP sites from various locations of the World's Oceans are compiled to get a picture to understand the variability of the concentration profiles and Mg/Ca, Sr/Ca profiles in the core sections due to different amount of diagenetic alterations and the different processes of diagenesis responsible for such variability. The purpose of such understanding is to investigate if there is any trace of seawater composition from the geologic past preserved as porefluids in the sediment cores. If we can back track the Mg and Sr seawater compositions in the geologic past, determination of paleotemperature using these elemental compositions of the biogenic carbonate will be more precise.

# **Mantle Structure beneath East Africa and Zambia from Body wave Tomography**

**Gabriel Mulibo**

Ph.D student, Post-comps

**Advisor: Andrew A. Nyblade**

R.W. Ferdinand, University of Dar Es Salaam, Tanzania

In this study, P and S travel time residuals from teleseismic earthquakes recorded on over 60 temporary AfricaArray seismic stations deployed in Uganda, Kenya, Tanzania and Zambia between 2007 and 2011 are being inverted, together with travel time residuals from previous deployments, for a 3D image of mantle wave speeds variations extending to a depth of 1200 km. Preliminary results show that at depths of 200 km or less, low wave speed anomalies are well developed beneath the Eastern and Western Branches of the East African Rift System. At deep depths, the low wave speed anomalies focus under the center and southern part of the East African Plateau and extend into the transition zone. At transition zone depths and within the top part of the lower mantle, the low wave speed anomaly shifts to the southwest beneath Zambia, indicating that the low wave speed anomaly is continuous across the transition zone and that it extends into the lower mantle. This result suggests that the upper mantle low wave speed anomaly beneath East Africa is connected to the African superplume anomaly in the lower mantle beneath southern Africa.

# Microbial community composition of marine subsurface samples from equatorial Pacific and Peru margin locations after multiple whole genome amplification methods

**Amanda Jean Martino**

Ph.D. Student, Pre-comps

**Advisor: Christopher House**

Matthew Rhodes, Penn State University

Jennifer Biddle, University of Delaware

Leah Brandt, Penn State University

The marine subsurface biosphere represents a frontier for the discovery of new microbial life, and for investigations of the extent, versatility and perseverance of life on Earth. However, there are many challenges in studying these communities, and the past couple decades have only begun to produce an understanding of this vast and complex ecosystem. Here, we examine microbial community composition of marine subsurface sediment samples from Peru Margin (ODP Leg 201) and Equatorial Pacific drill sites. DNA was sequenced with 454 metagenome sequencing technology after whole genome amplification with either a commercial phi 29-based kit, or a novel degenerate PCR-based method (RAMP<sup>1</sup>). Taxonomic analysis revealed that communities displayed distinctions based on site location, depth within the sediment column, and amplification technique employed. In the Peru Margin samples, communities were dominated by *Proteobacteria*, *Chloroflexi*, *Firmicutes*, *Euryarchaeota*, and *Crenarchaeota* phyla, while early analysis of the Equatorial Pacific samples showed some differences from this pattern (analysis currently ongoing). This study demonstrates the potential usefulness of the new whole genome amplification technique, RAMP, over commonly used commercial kits, particularly for very low biomass samples, but reinforces the caution that must be employed when utilizing any amplification technique prior to sequencing of environmental DNA samples.

[1] Martino, AJ, Rhodes, ME, Biddle, JF, Brandt, LD, Tomsho, LP, and House, CH (2012). Novel degenerate PCR method for whole genome amplification applied to Peru Margin (ODP Leg 201) subsurface samples. *Frontiers in Extreme Microbiology*. 3: Article 17.

# Oral Session One A: Environmental Geochemistry/Petrology

Saturday, March 17  
8:30-10:30 am, 114 EES

<b>Time</b>	<b>Presenter</b>	<b>Advisor</b>	<b>Title</b>
8:30	Kristina Peterson	Peter Heaney	A structure refinement for monoclinic hydrohematite
8:45	Ashlee Dere	Susan Brantley and Tim White	Quantifying shale weathering as a function of climate
9:00	Megan Carter	Susan Brantley	Soils as a record of long-term anthropogenic metal inputs in Marietta, Ohio
9:15	Heather Tollerud	Matt Fantle	The impact of climate and composition on playa surface roughness
9:30	Elizabeth Herndon	Susan Brantley	Quantifying the influence of vegetation on manganese mobilization and residence time in soils
9:45	Joe Orlando	Susan Brantley	Determining the depth of weathered corestone zone in the rain forest of Puerto Rico
10:00	Tiffany Yesavage	Susan Brantley	Mineral Weathering and Microbial Community Composition at a Mars Analog Site

# A structure refinement for monoclinic hydrohematite

**Kristina Peterson**

Ph.D. Student, Post comps

**Peter Heaney**

Jeffrey Post, Department of Mineral Sciences, Smithsonian Institution

In ferruginous soils, nano- to micro-scale hematite ( $\alpha$ -Fe<sub>2</sub>O<sub>3</sub>) plays a central role in redox processes and contaminant cycling. Hematite is known to incorporate structural OH<sup>-</sup> and water, and the requisite charge balance is achieved by iron vacancies. Prior researchers have suggested that the defective hematite structures form unique phases called “protohematite” (PH) and “hydrohematite” (HH) [1]. These phases are distinguished from stoichiometric hematite (SH) by their degree of hydration and iron deficiency. Furthermore, past infrared and Raman spectroscopic studies have assigned a lower-symmetry space group to PH/HH (*R3c*) relative to that of SH (*R-3c*) [2]. However, the existence and structure of these phases has been contentious, largely due to the lack of *in situ* X-ray diffraction data [3].

Here we present a new structure refinement for HH in a monoclinic space group (*I2/a*) using time-resolved X-ray diffraction (TR-XRD) data collected at the Advanced Photon Source (APS). Starting with ferric chloride solutions, we collected TR-XRD data during the *in situ* hydrothermal precipitation of akaganéite and its transformation to HH. Sealed quartz capillaries (1.0 mm diameter) were heated at 200 °C while XRD data were collected every 25 – 30 seconds. Rietveld refinements suggested a new monoclinic HH structure.

In our experiments, distinct peak splitting was observed in the hematite diffraction patterns, indicating a violation of the 3-fold rotational symmetry. The observed peak splitting in our data was outside the range calculated for sample displacement, and furthermore video footage obtained during the reaction showed particles uniformly convecting throughout the volume of the capillary. We therefore refined the structure in the various subgroups of *R-3c*. As the fit using *I2/a* was statistically no worse than that in lower symmetry groups, we selected this space group for our refinement. A monoclinic unit cell with parameters of  $a = 13.7493(15)$  Å,  $b = 5.0121(4)$  Å,  $c = 5.4418(6)$  Å,  $\beta = 147.6250(17)^\circ$  provided a good fit and significant reduction in  $\chi^2$  and  $R_{wp}$  relative to S.G. *R-3c*. Our results demonstrate that the *in situ* formation of the defective hematite phase, HH, was successfully captured. Moreover, HH is structurally distinct from SH and may form as a lower-symmetry monoclinic phase in soils.

[1] Dang *et al.* (1998) *Hyperfine Interact.* 117, 271-319. [2] Burgina *et al.* (2000) *J. Struct. Chem.* 41, 396-402. [3] Cornell and Schwertmann *The Iron Oxides*, 2<sup>nd</sup> ed. Wiley-VCH, Weinheim (2003).

# Quantifying shale weathering as a function of climate

**Ashlee Laura Denton Dere**

Ph.D. Student, Post comps

**Advisors: Susan Brantley and Tim White**

Rich April, Colgate University, Hamilton, NY

Brian Reynolds, Centre for Ecology and Hydrology, Bangor, Wales

Regolith, the mantle of physically, chemically, and biologically altered material overlying protolith (parent material), covers much of Earth's continents but the rates and mechanisms of regolith formation are not well quantified. Without this knowledge, predictions of the availability of soil to sustain agriculture for Earth's growing population are virtually impossible. In an effort to quantify the influence of climate on shale weathering rates, a transect of study sites has been established on Silurian shales along a climatic gradient in the northern hemisphere as part of the Susquehanna Shale Hills Critical Zone Observatory, PA. The climate gradient is bounded by a cold/wet end member in Wales and a warm/wet end member in Puerto Rico; in between, temperature and rainfall increase as sites extend south through New York, Pennsylvania, Virginia, Tennessee and Alabama. Soil and rock sampling and geochemical analyses were completed similarly at all sites to allow direct comparisons and eventual modeling of the shale weathering processes. The extent and depth of Na depletion, a proxy for feldspar weathering, is greater in higher mean annual temperature and precipitation regimes. Although very little Na is present in the transect shales, feldspar depletion is one of the deepest reactions documented in soil profiles and may therefore be a reaction that initiates the transformation of high bulk density unweathered parent material to lower bulk density regolith. Assuming that the rate of depletion can be described using an Arrhenius equation, an apparent activation energy for the dissolution of feldspar (Na depletion) is  $67.6 \text{ kJ mol}^{-1}$ . Using this apparent activation energy, all sites were rescaled to  $25 \text{ }^{\circ}\text{C}$  to attempt to quantify the influence of precipitation on feldspar weathering rates. Na release rates appear to increase exponentially as a function of mean annual temperature and linearly as a function of mean annual precipitation. Overall, data collected from soils across the transect will promote a better understanding of how climate changes can impact soil formation rates.

# **Soils as a record of long-term anthropogenic metal inputs in Marietta, Ohio**

**Megan Carter**

M.S. Student

**Advisor: Sue Brantley**

Atmospheric deposition of metals emitted by anthropogenic activities has been a significant source of metal loading into soils in the United States for more than 200 years. Eramet Marietta Inc., located in southeast Ohio, is one of the only ferromanganese refineries in N. America and one of the largest emission sources of manganese (Mn) into the atmosphere in the United States. Particulate emissions during production are up to 31-34% percent manganese oxide (MnO) by weight. These particles range in diameter from 0.05 to 0.4  $\mu\text{m}$ , making them both highly mobile and respirable. In order to assess the role of soils in Marietta as sinks for atmospherically-derived Mn, a series of soil cores from locations spanning a range of atmospheric Mn concentrations have been collected. In each core, Mn is enriched at the surface 2-6 times above parent material composition sampled at 1 m depth. Total added Mn over the depth of each core was calculated to be between 37 and 144  $\text{mg Mn/cm}^2$  of land area. While evidence of Mn inputs to soils exists, these inputs do not correlate with a model of atmospheric concentrations for the Marietta area. This may indicate that present-day modeled conditions differ from the relatively recent past. Assessing human exposure from either air or soil chemistry, alone, may be problematic.

# The impact of climate and composition on playa surface roughness

**Heather Tollerud**

Ph.D. Student, Post comps

**Advisor: Matthew Fantle**

Atmospheric mineral dust has a wide range of impacts, including the transport of elements in geochemical cycles, health hazards from small particles, and climate forcing via the reflection of sunlight from dust particles. For instance, dust inputs to the ocean potentially affect the iron cycle by stimulating natural iron fertilization, which could then modify climate via the biological pump. Also dust can transport nutrients over long distances and fertilize nutrient-poor regions, such as island ecosystems or the Amazon rain forest. However, there are still many uncertainties in quantifying dust emissions from source regions. One factor that influences dust emission is surface roughness and erodibility, since a weak, unconsolidated surface is more easily ablated by wind than a strong, hard crust. We are investigating the impact of processes such as precipitation, groundwater evaporation, and wind on surface roughness in a playa dust source region, the Black Rock Desert.

We find that water has a significant influence on surface roughness. We analyzed approximately 65 observations from ESA's Advanced Synthetic Aperture Radar (ASAR) instrument. An ASAR image indicates where the playa surface is smooth (on the scale of centimeters) and potentially very strong, and where it is rough and might be more sensitive to disturbance. In general, the playa is smoother and more variable over time relative to nearby areas. There is also considerable variation within the playa. While the playa roughness maps changed significantly between summers, over the course of each summer the playa surface maintained essentially the same roughness pattern. This suggests that there were no active processes during the summers that changed surface roughness. Images from NASA's MODIS instrument (1640 nm, band 6) delineate winter flooding on the playa. Years with more extensive flooding tend to result in a smoother playa, although areas with late season evaporation are relatively rough. This indicates that water disrupts the playa surface, reducing roughness, while drying can increase roughness. We also compared the distribution of surface roughness across the playa to playa composition. X-ray diffraction (XRD) of samples from the Black Rock Desert demonstrates that the playa surface is composed of approximately 30% quartz, 45% clays, 10% calcite, and 5% halite. Calcite and halite concentrations vary significantly between samples. We find that calcite concentrations are higher in smooth areas that have been inundated by water. Without an understanding of the surface processes associated with dust emission, it is difficult to model atmospheric dust, especially in the past or future when there is much less data for an empirical dust model.

# Quantifying the influence of vegetation on manganese mobilization and residence time in soils

**Elizabeth Herndon**

Ph.D. Student, Post comps

**Advisor: Susan Brantley**

Soils in industrialized regions can be enriched in trace metals due to inputs from atmospheric deposition. While much research targets the environmental transport of particularly harmful contaminants (e.g. Pb, Hg), a large suite of trace elements, including manganese, has been distributed across the Earth's surface and may impact ecosystem health and water quality. Mn, a primary component of many biogeochemical reactions, is enriched in soils throughout industrialized areas of Pennsylvania and the United States<sup>1</sup>. Here, we investigate factors affecting the mobility of various Mn-containing compounds in order to evaluate the residence time of Mn contamination in soils. We use a model soil system to quantify the influence of vegetation on rates of Mn transfer from soil components into water.

Soil mesocosms were established in a greenhouse setting in order to evaluate field processes under controlled conditions. One-gallon pots were filled with mineral soil collected from the Shale Hills Critical Zone Observatory (SHCZO), a forested watershed in central PA that has experienced Mn enrichment from industrial deposition. Red oak seedlings were planted in 46 pots to assess vegetation impacts, and 20 pots were left as non-vegetated controls. Pots either contained only mineral soil or were amended with aqueous Mn, Mn-rich organic matter, or Mn-oxides. Effluent was collected weekly and analyzed for major cations (Mn, Ca, K, Mg, Na, Fe, Al, P) to determine leaching rates. After 19 weeks, red oak leaves were harvested and chemically analyzed to determine uptake rates.

Vegetation was found to significantly increase the residence time of Mn in the soil mesocosms. In vegetated pots, uptake of Mn exceeded leaching by approximately 100-fold, and this effect of vegetation was more pronounced for Mn than for major plant nutrients (Ca, K, Mg, P). Additionally, Mn leaching was strongly reduced in vegetated pots relative to non-vegetated pots. Aqueous Mn additions were strongly retained in the mineral soil (>95%) but were still leached more rapidly than Mn from other sources. In total, Mn leaching rates decreased from aqueous > Mn-oxide > mineral soil sources. The addition of Mn-rich organic matter resulted in a decrease in Mn leaching, which suggests adsorption of soluble Mn onto solid-phase organics, and may contribute to Mn retention in soils.

<sup>1</sup>Herndon E.M., Jin L., Brantley S.L. (2011) Soils reveal manganese enrichment from industrial inputs. *Environ. Sci. Technol.* 45(1), 241-247.

# **Determining the depth of weathered corestone zone in the rain forest of Puerto Rico**

**Joseph Orlando**

Ph.D. Student, Pre-comps

**Advisor: Sue Brantley**

Sue Brantley, Pennsylvania State University

One of the fastest documented weathering rates of silicate rocks is found in the Rio Icacos watershed, a humid tropical ecosystem in the Luquillo Mountains in northeastern Puerto Rico. Although the tropics only cover about 25% of the earth's land surface, they provide 50% of the water, 38% of dissolved ions, and 65% of the dissolved silica that enters the oceans from land. Atmospheric concentrations of CO<sub>2</sub> are also influenced by the weathering of silicate rocks. The Rio Icacos watershed is underlain primarily by the Tertiary Rio Blanco quartz diorite intrusion with a contact metamorphic hornfels topping peaks in the north and eastern portions of the watershed. While the weathering of the quartz diorite has been extensively studied, there is a lack of understanding about how the weathering of the hornfels is taking place. The quartz diorite weathers in a typical spheroidal rindlet pattern and the hornfels weathers into more angular blocks. The zone where corestones are forming, here called the corestone routing zone CRZ, is thought to be where the groundwater is flowing and reacting with the bedrock.

Drilling plans have been arranged in the quartz diorite and in the hornfels in order to collect regolith samples, solid rock cores, and to place water samplers in zones where water is flowing in fractures in the bedrock. The drilling will take place as near to ridgetops as possible. A ridgetop can be thought of as a one dimensional weathering engine where erosion does not add material as in a midslope or lower regime. For this reason, drilling on a ridgetop can give valuable information that will help determine weathering rates and chemical changes at the regolith/bedrock interface. Previous drilling on the quartz diorite showed the regolith/bedrock interface to be at about 4.8m depth below ground surface at location nearby to the Rio Icacos.

We hypothesize that the water table in the quartz diorite will be found near the CRZ which is thought to be about 30m below ground surface at the proposed drilling location. At the hornfels location, this depth is thought to be at about 25m below ground surface at the proposed drilling location.

# Mineral Weathering and Microbial Community Composition at a Mars Analog Site

**Tiffany Yesavage**

Ph.D. Student, Post comps

**Susan Brantley**

Laura Liermann, Penn State University

Istvan Albert, Penn State University

Elisabeth Hausrath, The University of Nevada, Las Vegas

Although weathering in cold, dry climates is often assumed to be dominated largely by physical weathering, evidence for chemical weathering has also been noted at different sites to varying extents. We are investigating mineral weathering patterns and microbial community composition in Svalbard, an archipelago that lies above the Arctic Circle. Due to its cold, dry climate and basaltic composition, Svalbard is considered to be a Mars analog site. The specific study site under investigation, the Sverrefjell volcano, consists of weathering basalt lava flows that are Quaternary in age and have been weathering since deglaciation commenced 10,000 years ago. Regolith samples for this study were collected from two different types of sites, which included fractured rock and loose regolith.

Although several interpretations are possible, chemistry data from regolith samples suggest that chemical weathering has occurred after only 10,000 years of weathering. In order to understand the role that colloidal dispersion may play in soil development, colloidal dispersion experiments were performed both under oxic and anoxic conditions. Results from these experiments indicate that Fe, Al, S and P are dispersed primarily as particles larger than 35 nm. In contrast, elements such as Mg, Na and Ca are dispersed solely in the <2 nm size fraction. 454 pyrosequencing was performed upon regolith samples collected from five different locations on the volcano. Consistent with other studies of microbial soil composition, the results indicate that the predominant groups of organisms present in Svalbard regolith include *Proteobacteria*, *Actinobacteria*, *Bacteroidetes* and *Acidobacteria*.

# Oral Session One B: Geodynamics/Petrology

Saturday, March 17  
8:30-10:30 am, 116 EES

<b>Time</b>	<b>Presenter</b>	<b>Advisor</b>	<b>Title</b>
8:30	Bryan Kaproth	Chris Marone	Fault gouge evolution during rupture and healing: Continual active-seismic observations across laboratory-scale fault
8:45	Marco Scuderi	Chris Marone	Physicochemical Processes of Frictional Healing and Lithification: Effects of Water on Stick-Slip Stress drop and Friction in Synthetic Fault Gouge
9:00	Travis Call	Terry Engelder	Effect of lithology and bedding plane orientation on geomechanical properties of Middle Devonian core samples
9:15	Christine Regalla	Don Fisher	An alternative mechanism for forearc subsidence along the Northeast Japan erosive margin?
9:30	Halldor Geirsson	Peter LaFemina	Deep magma accumulation at a rift – transform intersection: geodetic constraints on the magma plumbing system at Hekla volcano, Iceland
9:45	Daisuke Kobayashi	Peter LaFemina	Effects of Cocos Ridge Collision on the Western Caribbean: Is there a Panama Block?
10:00	Matthew Herman	Kevin Furlong	Constraining Earthquake Processes During the 2010-2012 Canterbury Earthquake Sequence
10:15	Alicia Cruz-Urbe	Maureen Feineman	Rutile-titanite reaction rates from diffusion of Nb in rutile
10:30	Megan Pickard	Tanya Furman	Petrogenesis of alkaline mafic rocks from Sivas, Central Anatolia: New insight into ancient continental assembly and break-up

# **Fault gouge evolution during rupture and healing: Continual active-seismic observations across laboratory-scale fault**

**Bryan M. Kaproth**

Ph.D. Student, Post comps, Petroleum related

**Advisor: Chris Marone**

Our understanding of rupture and healing processes within natural faults is progressing with seismology's recent focus on crustal velocity change through time. We report on laboratory studies designed to investigate fault processes during seismic (slip) and interseismic (quasi-static) periods using active-source acoustics. We directly build on these recent seismology studies, which probe natural-faults using a range of sources (i.e. repeating earthquakes, noise correlation, etc.). Many of these observations are clearly related to the seismic cycle. However owing to the remote nature of seismic data, linking these observations to their mechanical causes (e.g., contact bonding, frictional healing, crack closure, etc.) is not always clear. These studies often rely on laboratory work relating elastic properties to load, damage, or porosity, which can only provide a piecemeal understanding of the seismologic data. Our study addresses the need for high-quality observations of fault zone elastic properties under carefully controlled laboratory conditions, as motivated by recent seismic observations.

We shear layers of synthetic and natural fault gouge using the double-direct shear configuration in a servo- hydraulic testing machine. The stationary forcing blocks contain embedded shear-wave PZTs (0.5 MHz), and we conducted detailed calibrations to determine elastic properties of the system. Throughout each friction experiment, we pulsed one PZT (900 V) and recorded 100 stacked waveforms every 2 s. We sheared layers of brine saturated halite (layer thickness = 5 mm, particle size = 75-250  $\mu\text{m}$ ) to steady-state residual strength and then conducted slide-hold-slide tests at 15 MPa normal stress, 23° C. Previous work shows that fault healing occurs by pressure-solution under these conditions. In a representative test, porosity decreased from 10.0 to 5.7 % during hold (interseismic) periods of 10,000 s, and porosity recovered back to 11.0% during reloading and subsequent shear (seismic slip). Over this seismic-interseismic cycle, P-wave velocities,  $\alpha$ , ranged between 2.8 to 2.0 km/s and S velocities,  $\beta$ , ranged between 2.1 to 1.4 km/s. In particular, these velocities clearly increase linearly with log time during the interseismic period. We find that seismic velocity is determined primarily by porosity change and stress. Experiments designed to isolate these individual effects show that for every 1% of porosity lost,  $\alpha$  and  $\beta$  increase by 1.4-1.8 % and 2.7-3.0 %, respectively. And for every MPa of shear stress increase,  $\alpha$  and  $\beta$  increase by 1.0-1.4 % and 1.4-2.2 %, respectively. We resolve hysteresis in these relationships between the seismic and interseismic intervals, but this tends to be small. Dynamic bulk- and shear-modulus as well as p- and s-wave amplitudes exhibit similar load and porosity dependencies. As applied to monitoring of tectonic faults,

our data suggest that for each percent increase in  $\alpha$  or  $\beta$ , fault gouge strengthens on the order of 0.022% or 0.029%, respectively.

## **Physicochemical Processes of Frictional Healing and Lithification: Effects of Water on Stick-Slip Stress drop and Friction in Synthetic Fault Gouge**

**Marco Scuderi**

Ph.D. Student, pre-comps

**Advisor: Chris Marone**

Earthquakes are dynamic phenomena characterized by slip instability along a preexisting zone of weakness (fault zone) within more competent rock. Fault zones are characterized by granular and clay-rich wear material (fault gouge) produced by dynamic and quasi-static slip processes. The mechanical strength, frictional stability, and seismic potential of a fault are strongly influenced by the evolution of grain contacts within the fault zone. In this context, water plays an important role at mineral surfaces and within contact junction via processes such as hydrolithic weakening, adsorption/desorption and pressure solution. To investigate the role of water in faulting, we performed shear experiments using synthetic fault gouge as a function of relative humidity (RH) and normal stress ( $\sigma_n$ ). We sheared layers of soda-lime glass beads of known initial grain size (dia. 105 to 149  $\mu\text{m}$ ) in a double direct shear configuration. Normal stress was kept constant during shear at 5 MPa. Shear stress ( $\tau$ ) was applied via a constant displacement rate at the layer boundaries, and shearing velocity was varied from 0.3 to 300  $\mu\text{m/s}$  via a sequence velocity steps. Careful calibration of apparatus stiffness plus an on board DCDT, mounted directly across the shear zone, were used to measure slip velocity of the fault zone. During each experiment, RH was kept constant at values of 5, 50 30 and 100%. Our experiments were conducted in the stick-slip sliding regime. We find that maximum friction  $\mu_{\text{max}}$  increases systematically with increasing RH, in contrast to previous results for angular quartz and nominally-bare surfaces. In agreement with previous studies, our results indicate that frictional behavior of simulated fault gouge is strongly influenced by RH and contact properties. Post experiment SEM analysis of glass beads reveals that the real contact area at the grain junction increases as a function of RH%. In particular we document that for RH = 5% the contact radius is 9.1  $\mu\text{m}$ , and with increasing humidity it evolves to 12.1  $\mu\text{m}$  at RH = 50% and 19.6  $\mu\text{m}$  at RH = 100%. Moreover, analyses of the shape of the contacts reveal an evolution from elastic to elasto-plastic deformation at the grain junctions. Our results confirm that water activated chemical processes, such as hydrolithic weakening or eventually pressure solution, act at the grain junctions, the area of contact between particles bduring the elastic and elasto-plastic loading (inter-seismic period), increasing the frictional strength of synthetic fault gouge.

# **Effect of lithology and bedding plane orientation on geomechanical properties of Middle Devonian core samples**

**Travis Call**

M.S. Student, Petroleum related

**Terry Engelder**

Gas production from the Middle Devonian-age Marcellus shale of the Appalachian Basin relies on hydraulic fracture stimulation of a low permeability, organic-rich reservoir. In addition to in-situ stress, the geomechanical properties of the gas shale and bounding strata play an important role in fracture growth during stimulation. Four-point bend tests of rock core samples provide an understanding of fracture growth through the calculated values of fracture toughness, elastic modulus, and tensile strength for several lithofacies throughout the Marcellus and associated strata. The surface roughness of the fractured sample is then quantified with an optical profilometer and the correlation between fracture toughness and surface roughness is determined. These geomechanical properties influence the propagation, size, and conductivity of hydraulically induced fractures. Knowing how these parameters change throughout the Marcellus shale could improve the design and efficiency of wellbore placements and hydraulic fracture treatments. Also of interest is the effect bedding plane orientation has on the geomechanical behavior of the core samples. Samples are loaded with both arrester and divider bedding plane geometries (from Schmidt, 1977) to examine the variation in geomechanical properties caused by the orientation of bedding planes with respect to the loading direction. Results indicate a significant increase (up to 30%) in fracture toughness for the divider geometry of finely laminated lithofacies. Conversely, lithologies without prominent bedding planes show little difference in fracture toughness between the divider and arrester geometries. Tensile strength results show a wide range of values which can be attributed to the lack of a consistent defect size along which the sample fails (i.e. the small notch cut into fracture toughness samples). Furthermore, the data shows variability in the properties of the three Marcellus shale members (Oatka Creek, Purcell, and Union Springs) and the bounding strata as a function of both lithology and bedding plane orientation.

# **An alternative mechanism for forearc subsidence along the Northeast Japan erosive margin?**

**Christine Regalla**

Ph.D. Student, Post comps

**Advisors: Don Fisher and Eric Kirby**

Additional authors: Kevin Furlong

New data from the northeast Japan erosive margin demonstrate that variations in vertical motions are temporally linked with changes in lower plate convergence rate. Nearly half the world's subduction zones are non-accretionary and are characterized by long-term forearc subsidence. Subsidence along these margins has been interpreted to be the result of basal tectonic erosion, in which removal of upper plate material along the subduction zone interface drives mass loss and subsidence of the outer forearc. The processes and mechanisms that initiate and sustain forearc subsidence along these erosive margins, however, are not well understood. Here, we evaluate the relationship between deformation within the upper plate along the northeastern Japan convergent margin and temporal variations in relative plate convergence. The initiation of shortening along reverse faults in the forearc (Futaba and Oritsume faults) is constrained by new and existing U-Pb ages from tephras in pre-growth and growth strata that bracket the initiation of thrust displacement to ~5.6 to ~3.9 Ma for the Futaba and 5.9 to 4.8 Ma for the Oritsume fault. In addition, the hanging walls of both structures are characterized by thick sequences of Miocene sediments that are absent in the footwall, suggesting that these structures are reactivated Miocene normal faults. A regional synthesis of deformation reveals that the timing of deformation along these forearc structures is part of a margin-wide reorganization deformation. In addition, published subsidence histories from offshore sediments exhibit a similar transition, from Miocene subsidence to Plio-Quaternary uplift in the outer forearc. Updated analyses of Pacific-Honshu plate convergence rates during the Cenozoic reveals that the initiation of forearc extension and subsidence is coeval with a two to three fold increase in margin-perpendicular convergence rate between 30-20 Ma, and that the transition to compression during the Pliocene occurred during a period of relatively constant convergence rate. The temporal correlation between deformation along upper plate faults, forearc subsidence, and lower plate convergence rates suggests that vertical motions of the forearc during the Cenozoic are likely governed by changes in lower plate kinematics. An increase in convergence rate can induce changes in slab geometry at shallow depths, which, in turn, may drive upper plate subsidence and extension. These results suggest that subsidence along the northeast Japan margin, previously attributed to basal tectonic erosion, could result from plate boundary dynamics.

# Deep magma accumulation at a rift – transform intersection: geodetic constraints on the magma plumbing system at Hekla volcano, Iceland

**Halldor Geirsson**

Ph.D. Student, Pre-comps.

**Advisor: Peter LaFemina**

Matthew Travis, Penn State

Erik Sturkell, University of Gothenburg

Thora Arnadottir, University of Iceland

Freysteinn Sigmundsson, University of Iceland

The majority of volcanoes on Earth are located at actively deforming plate boundaries. The magma sources responsible for volcanic deformation have been found to be at depths ranging from within the volcanic edifice down to at least 25 km. In this study GPS-geodetic data are used to investigate surface deformation caused by a magma source at Hekla volcano, Iceland. Hekla is one of Iceland's most active volcanoes with 18 documented eruptions in the last millennium. The volcano is located at an inside corner of a highly magmatic rift-transform intersection on the Mid-Atlantic Ridge. The proximity of Hekla to the plate boundary, active fault zones, other deforming volcanoes in addition to glacial rebound and localized subsidence at Hekla, results in a complex deformation field. Taking all these complications into account, either by applying corrections or by modeling the deformation sources directly, the location, depth, geometry of the source, and magma supply rate for Hekla's magma chamber are estimated.

The results demonstrate the importance of considering all the various deformation sources around Hekla, because the horizontal surface deformation rate caused by magma accumulation at Hekla is less than 5 mm/yr, which is relatively small compared to typical uncertainties of 1 mm/yr and the 19 mm/yr spreading rate between the North American and Eurasian plates. The results imply that despite the divergent tectonic regime in Iceland, Hekla's magma chamber is not dominantly elongated along the plate boundary, however, it is well represented by a spherical shape. Solving for the location of the rift- and transform zones, the axis of spreading is estimated to be 20 km east of Hekla. The best-fitting magma source at Hekla is centered  $2.4^{+1}_{-3}$  km west of the summit and the depth of the center of the magma chamber is  $23^{+5}_{-2}$  km. This is the greatest depth yet observed for any deformation source in Iceland. The observed depth places the magma source for Hekla at the deepest levels of the crust or at the crust-mantle boundary. The magma inflow rate needed to explain the surface deformation is  $0.020^{+0.011}_{-0.003}$  km<sup>3</sup>/yr, which is comparable to the average effusive flux from the volcano over the past millennium.

# Effects of Cocos Ridge Collision on the Western Caribbean: Is there a Panama Block?

**Daisuke Kobayashi**

M.S. Student

**Advisor: Peter LaFemina**

Halldór Geirsson, Pennsylvania State University, PA

Eric Chichaco, University of Panama, Panama City, Panama

Antonio A. Abrego M., Panama Canal Authority, Panama City, Panama

Donald M. Fisher, Pennsylvania State University, PA

Eduardo I. Camacho, University of Panama, Panama City, Panama

Hector Mora-Páez, INGEOMINAS, Bogota, Colombia

It has been recognized that the subduction and collision of the Cocos Ridge, a 2 km high aseismic ridge standing on >20 km thick oceanic crust of the Cocos plate, has profound effects on upper plate deformation and block kinematics in southern Central America. Recent studies of Global Positioning System (GPS) derived horizontal velocities relative to the Caribbean Plate showed a radial pattern centered on the Cocos Ridge axis where Cocos-Caribbean convergence is orthogonal. Models of the full three-dimensional GPS velocity field and earthquake slip vectors demonstrate low mechanical coupling along the Middle America trench in Nicaragua and El Salvador, and a broad zone of high coupling beneath Osa Peninsula, where the Cocos Ridge intersects the margin. These results suggest that Cocos Ridge collision may be the main driver for trench-parallel motion of the fore arc to the northwest and for uplift and shortening of the outer fore arc in southern Central America, whereby thickened and hence buoyant Cocos Ridge crust acts as an indenter causing the tectonic escape of the fore arc. These studies were not able to constrain well the pattern of surface motion on the Panama block due to a lack of GPS stations.

Utilizing new GPS data from a reinforced network in southern Costa Rica and Panama, we investigate the effects of Cocos Ridge collision. We invert the full three-dimensional GPS data and earthquake slip vectors to solve for relative block rates, Euler vectors of the blocks of interest, and magnitude and pattern of mechanical coupling on block bounding faults. Geologic and geophysical data and published earthquake relocations are used to define plate and block boundaries and fault geometries. In this study, we test different block boundaries separating the Central American fore arc (CAFA) and Panama block (PB). Model results indicate high coupling (>50%) along Osa and Nicoya Peninsulas with good resolution. The best fit model suggests the migration of the CAFA and PB at rates of 10–14 mm a<sup>-1</sup> and 6–9 mm a<sup>-1</sup>, respectively, indicating upper plate deformation due to Cocos Ridge collision that must be accounted for in seismic hazard assessments.

# Constraining Earthquake Processes During the 2010-2012 Canterbury Earthquake Sequence

**Matthew Herman**

M.S. Student

**Advisor: Kevin Furlong**

Robert Herrmann, Saint Louis University

Harley Benz, National Earthquake Information Center, USGS

On September 3 2010, a M7.0 earthquake ruptured 100 kilometers southeast of the Alpine Fault across the Canterbury Plains on South Island, New Zealand. Since then, New Zealand GNS has recorded over 10,000 aftershocks, including three destructive ~M6.0 events near Christchurch. Because there are no apparent active tectonic structures and no major seismicity has been recorded prior to September 2010, we treat the Canterbury sequence as an intraplate earthquake sequence. We compare it to typical plate boundary earthquake sequences, where rigid blocks are displaced past each other, and the displacement controls the slip direction and the stress accumulation rate on faults.

We determined best-fitting double couple solutions for 139 earthquakes with moment magnitude  $M_w \geq 3.7$  in the Canterbury earthquake sequence. Each double couple solution includes two nodal planes and slip directions, allowing us to characterize earthquake faulting geometries and kinematics. Additionally, the solutions yield P- and T-axis orientations, which are inferred to represent the orientations of stresses driving the earthquakes. The kinematics of the Canterbury aftershocks differ from those predicted for plate boundary event aftershocks: slip vector orientations change systematically along strike and cannot be completely described by relative motion between two rigid blocks. Despite the variations in slip direction, most of the aftershocks have nearly the same maximum stress orientation, consistent with regional stress orientations. There is no clear evidence for major stress changes, even near a fault segment with ~5 meters of slip during the September main shock. We conclude that stress in the Canterbury Plains intraplate setting was accumulated by nearly uniform regional deformation rather than block displacement past a locked fault.

# Rutile-titanite reaction rates from diffusion of Nb in rutile

**Alicia Cruz-Uribe**

Ph.D. Student, Post comps

**Advisor: Maureen Feineman**

Thomas Zack, Universität Mainz

Reaction rates for the rutile to titanite transition have been determined in garnet amphibolite and retrogressed eclogite from Catalina Island, CA; Tromsø, Norway; and North Qaidam, China. Trace element concentrations in rutile and titanite were determined by LA-ICP-MS. Niobium profiles across rutile grains (210-1275  $\mu\text{m}$ ) show evidence for Nb back-diffusion into rutile during titanite growth at the grain boundary. Zr-in-titanite thermometry indicates  $760\pm 28$  °C for Catalina,  $699\pm 27$  °C for Tromsø, and  $671\pm 18$  °C for N. Qaidam. Experimentally-determined diffusion coefficients for Nb in rutile were used to model Nb diffusion in rutile using a simple 1-D moving interface diffusion model.

Rutile-titanite reaction rates for Catalina range from  $1.14\text{--}5.17\times 10^{-6}$   $\text{a}^{-1}$ , which correspond to overall reaction timescales of 194–876 k.y. Reaction rates for N. Qaidam are  $1.07\text{--}1.85\times 10^{-7}$   $\text{a}^{-1}$  (5.4–9.3 m.y.), and for Tromsø are  $1.40\text{--}1.92\times 10^{-8}$   $\text{a}^{-1}$  (~50–70 m.y.). Surface area normalized reaction rates average  $3.27\times 10^{-6}$   $\text{g}/\text{cm}^2/\text{a}$  for Catalina,  $2.92\times 10^{-7}$   $\text{g}/\text{cm}^2/\text{a}$  for N. Qaidam, and  $9.96\times 10^{-8}$   $\text{g}/\text{cm}^2/\text{a}$  for Tromsø. These rates extend the range of previously determined field-based regional metamorphic reaction rates to higher temperatures, allowing us to extend the parameterization of the rate law for regional metamorphic reactions.

# **Petrogenesis of alkaline mafic rocks from Sivas, Central Anatolia: New insight into ancient continental assembly and break-up**

**Megan Pickard**

Ph.D. Student, Post comps

**Advisor: Tanya Furman**

Tanya Furman, Penn State

Biltan Kürkcüoğlu, Hacettepe University

Barry B. Hanan, San Diego State University

Kaan Sayit, San Diego State University

Alkaline mafic lavas are a common feature of intraplate extensional volcanic settings. We examine mafic lavas from Sivas, Central Anatolia, in order to understand controls on their genesis in a setting with a complex tectonic history extending over the past 1.3 billion years. Continental assembly and break-up, both associated with geochemical modifications to the associated lithosphere, has long played a significant role in Anatolia. The present tectonic regime consists of a complex juxtaposition of rift, strike-slip, and transtensional faulting and an overall WSW movement of the continental microplate.

We identify two groups of alkaline lavas that record different petrogenetic histories. Select incompatible trace element variations (e.g., Ti, Zr) indicate that abundant basalts and basaltic andesites (BBA) evolved by fractional crystallization of a frequently-erupted parental magma with ~9 wt.% MgO. The BBA lavas have overall smooth primitive mantle normalized incompatible trace element patterns that suggest derivation from a source region geochemically similar to that of ocean island basalts. In contrast, basanites erupted over a small geographic area show little fractionation but rather represent individual magma batches with different degrees of partial melting. These lavas exhibit enrichments in Ba, Th, and U and depletions in Rb, Hf and Ti that are characteristic of melts derived from metasomatized lithosphere. Pb abundances in both groups are anomalously high, though this feature is more pronounced in the basanites, suggesting interaction with a Pb-rich continental component.

In general, Sr-Nd-Hf radiogenic isotopic signatures of the BBA lavas are less radiogenic than those measured in the basanites. The BBA and basanite groups overlap in eNd-eHf isotope space, plotting on and above the mantle array between data fields for oceanic basalt-like and continental lithosphere-like compositions. The least radiogenic BBA lavas ( $^{87}\text{Sr}/^{86}\text{Sr}$  0.7040-0.7044;  $^{143}\text{Nd}/^{144}\text{Nd}$  0.51278-0.51280) approach compositions of asthenospheric melts. Radiogenic Pb isotope compositions of both groups plot within the range of Indian MORB. Nd model ages of Sivas lavas are consistent with a DUPAL-like source region with ~1.3 Ga continental lithosphere affinity.

# Oral Session Two A: Paleontology

Saturday, March 17  
11:00 am-12:15 pm, 114 EES

<b>Time</b>	<b>Presenter</b>	<b>Advisor</b>	<b>Title</b>
11:00	Lauren Milideo	Russ Graham	Wolf Den vs. Landscape: Actualistic Taphonomy of Different Site Types
11:15	Jon Schueth	Tim Bralower	First-come, First-served: The Role of Survivor Incumbency in the Evolution of Calcareous Nannoplankton after the Cretaceous/Paleogene (K/Pg) Mass Extinction
11:30	Sara Elliott	Peter Wilf	Characterizing a Pre-Colonial Piedmont Riparian Forest using Sub-Fossil Leaves: West Branch Little Conestoga Creek, Southeastern Pennsylvania
11:45	Cassi Knight	Peter Wilf	Rare leaf fossils of Monimiaceae and Atherospermataceae (Laurales) from Eocene Patagonia: biogeography of ancient southern rainforest lineages
12:00	Max Christie	Mark Patzkowsky	The Ecological Effects of Extinction

# **Wolf Den vs. Landscape: Actualistic Taphonomy of Different Site Types**

**Lauren Milideo**

Ph.D., Pre-comps

**Advisor: Russ Graham**

Russ Graham, Penn State University, University Park, PA

The fossil record is a rich source of data from which paleontologists may extract paleoecological data. The temporal and spatial scale on which these fossil assemblages formed may vary widely, but such differences are not always immediately obvious. The nature of various taphonomic pathways is dependent upon factors that may sort, alter, and bias bone accumulations, resulting in a fossil assemblage that differs taxonomically or quantitatively from the original ecological community. It is thus necessary to identify and, if possible, remove this overprint, as underlying paleoecological data may otherwise be obscured or distorted. Hence, placing fossil assemblages into a taphonomic framework is an essential first step in paleoecological analysis.

Taphonomic alteration may occur via predator selection of specific prey taxa or skeletal elements; predators may preferentially remove certain bones from the landscape and deposit them at dens. This creates diverse assemblages, leaving differential damage on bones and providing a means of identifying the type of site from which they are derived. Thus study of modern bones from different types of sites will provide a means of identifying what taphonomic biases impacted a bone assemblage, and how it may have been altered as a result. Here we present a comparison between den- and landscape-derived modern bone assemblages, specifically caribou bones from wolf dens in Nunavut, Canada, and bison bones from Wind Cave National Park, South Dakota. We examine damage to the bones resulting from scavenging and feeding activities, as well as spatial distribution patterns of the bones. Initial results indicate several differences between these sites. The wolf den assemblage shows more substantial and frequent carnivore damage, including toothmarks and fracturing. Preliminary spatial analysis also suggests a difference between the distributions of bone deposits between these two site types. This analysis is part of an ongoing study to identify quantifiable taphonomic differences between these assemblages, and more den- and landscape-derived bones will be analyzed and compared as the project continues. This study will provide a means of identifying, and accounting for, taphonomic alterations to fossil bone assemblages – an important factor in drawing well-founded paleoecological conclusions.

# **First-come, First-served: The Role of Survivor Incumbency in the Evolution of Calcareous Nannoplankton after the Cretaceous/Paleogene (K/Pg) Mass Extinction.**

**Jon Schueth**

PhD Student, Pre-comps

**Advisor: Tim Bralower**

Mark Patzkowsky, Penn State

Sjijun Jiang, Jinan University, China

The mass extinction at the Cretaceous/Paleogene (K/Pg) boundary (65.68 million years ago) has been well documented across marine and terrestrial communities with an extensive fossil record. The lowermost Paleogene provides a unique setting to study how communities recovered from near annihilation. Calcareous nannoplankton have a detailed fossil record over the boundary, and 93% of nannoplankton species went extinct at the K/Pg. While this extinction is well documented, very little has been done to investigate the evolutionary dynamics of the nannofloral recovery.

This work specifically investigates where key nannoplankton lineages developed, how newly evolved species became abundant globally and the role survivors played in the recovery. We focused on two locations, the North Pacific and South Atlantic, because of the well constrained age control at these sites. Key lineages of nannoplankton appear to evolve in the North Pacific before the South Atlantic perhaps due to low survivor abundance and a lack of competition for resources in the Northern Hemisphere. Survivors rapidly diversified after the boundary in the South Atlantic, but this diversification was followed by relatively little change in diversity for hundreds of thousands of years. We hypothesize that, in the Southern Hemisphere, survivors filled available niche space and developed into an incumbent assemblage. Incumbency limited the diversification in the South Atlantic and made it more difficult for the new Paleogene nannoplankton to disperse into southern environments. The transition to a truly global Paleocene nannofloral assemblage occurred at roughly the same time as the recovery of the biologic pump and surface ocean ecosystems. We propose that the recovery of the biologic pump lessened survivor abundance and allowed for the key Paleogene lineages to become abundant globally.

# Characterizing a Pre-Colonial Piedmont Riparian Forest using Sub-Fossil Leaves: West Branch Little Conestoga Creek, Southeastern Pennsylvania

Sara Elliott  
M.S. Student

Advisor: Peter Wilf

Reconstruction of a Piedmont wetland and adjacent hillslope plant community using sub-fossil leaves from Lancaster County, PA shows a significant shift in stream bank vegetation since colonial settlement. Leaf mat deposits occur within an organic-rich hydric soil immediately underlying silty remnant "legacy sediments" derived from colonial agricultural practices beginning in the 18th century. Between 1 and 5 meters of these silty sediments accumulated in slackwater ponds behind milldams, entombing the hydric soil, altering the natural floodplain, and causing subsequent riparian vegetation shifts. Because leaves in fine-grained sediments are rarely deposited far from their source, the sub-fossil leaves presumably represent the woody plant taxa originally associated with these pre-colonial stream profiles, before the alteration of stream channel patterns from anabranching systems with adjacent hillslopes to the "riffle and pool" meanders observed today.

Specimens were collected from Denlinger's Mill on West Branch Little Conestoga Creek, part of the larger Susquehanna and Chesapeake watersheds. Blocks of hydric soil were removed, and leaf remains were separated from mud using alternating baths of HCl and KOH until most siliciclastic and organic matter was eliminated. Specimens were then mounted on glass slides and examined using fluorescence microscopy. Many specimens are identifiable to species level based on leaf morphology, vein architecture, and cuticle features such as trichome types and stomatal configuration. Preliminary data indicate a majority of facultative non-wetland and upland species presumed to be derived from the adjacent hillslope, including an abundance of *Fagus grandifolia* (American Beech), *Quercus* spp. (oaks), and various family Betulaceae (Hornbeam and birches). This initial suggestion of a mesic mixed hardwood forest contrasts with the secondary disturbed riparian forest observed adjacent to the creek today, which is dominated by *Acer negundo* (Box Elder Maple) and *Acer saccharum* (Sugar Maple). Efforts will be continued to accurately constrain the original community and ecosystem type of this area, eventually leading to more effective stream restoration and conservation efforts in the future.

# Rare leaf fossils of Monimiaceae and Atherospermataceae (Laurales) from Eocene Patagonia: biogeography of ancient southern rainforest lineages

Cassi Knight

M.S. Student

Advisor: Peter Wilf

Two Eocene fossil localities, Laguna del Hunco (LH, 52.2 Ma) and Río Pichileufú (RP, 47.7 Ma), from Patagonia, Argentina have some of the most diverse fossil floras known. They represent angiosperm-dominated Gondwanan rainforests and have been the focus of many paleontological and geological studies. Here, I focus on a portion of the floras that has received little attention: rare, toothed fossil leaves with affinities to the magnoliid order Laurales, representing the basal families Atherospermataceae and Monimiaceae. These ancient lineages currently exhibit broad, often disjunct southern distributions and thus hold much interest for Gondwanan biogeography. However, their records are exceptionally scarce, in that only ~14 different fossil species are reported between these two families. The majority of these species are based on fossil wood, with only six represented by leaf impressions. The fossil wood record has low taxonomic precision, but recently has been reviewed and revised. The leaf macrofossil record prior to the Neogene, however, is in need of critical revision because most of the generic and familial assignments are incorrect. My purposes are to: 1) evaluate the presence of the families in Eocene Patagonia from new material by revising one fossil species and describing another; 2) determine modern genera showing the closest affinities; and 3) use the results to improve current understanding of Laurales biogeography. The first fossil species, *Laurelia guiñazui* Berry 1935, was originally described from RP and placed in Monimiaceae. Subsequently, *Laurelia* (South America and New Zealand) was assigned to Atherospermataceae. I report 16 new fossil specimens of *L. guiñazui* from LH and RP with greater preserved detail than in the syntypes. From this material, I support placement of *L. guiñazui* in Atherospermataceae, but not in any living genus, based on several typical characters: low leaf rank and vein density, acute basal secondaries, brochidodromous secondaries, and large, glandular, highly irregular, compound teeth. Evaluation of this fossil species, based on character scoring, suggests its closest affinity is to species in the living genera *Daphnandra*, *Doryphora* (both Australia), *Laureliopsis* (Chile and Argentina), and *Laurelia* (New Zealand and Chile). The second fossil species is represented by a single specimen from LH and is undescribed. It exhibits distinct ‘Monimioid’ teeth and other features that allow confident placement in Monimiaceae. Among extant genera, I note strongest similarity to *Wilkiea* (Australia) based on: low leaf rank, basally thickened midvein, strongly brochidodromous secondaries with basal pair acute, and small, closely spaced glandular teeth. This appears to contrast with molecular analyses, which place the divergence of the clade containing *Wilkiea* in Australasia between 16 and 38 Ma (Renner et al., 2010. *J. Biogeography* 37:1227). The affinity of the fossil to living *Wilkiea* implies that this lineage may be much older and have a much broader biogeographic history across Gondwana. This study significantly improves the fossil record of two early-diverging Laurales families by establishing what are probably their most reliable pre-Neogene occurrences, in Eocene Patagonia, at great modern distance from many of their closest living relatives.

# The Ecological Effects of Extinction

**Max Christie**

PhD. Student, Pre-comps

**Advisor: Mark Patzkowsky**

The ecological impacts of extinction are often measured in terms of the taxa lost; however, previous work has shown that patterns of taxonomic loss may differ from the loss of functional units in an ecosystem. Functional diversity is an important part of ecosystem stability, and should also be considered in order to understand the effects of extinction on ecological change.

I quantify the relationship between taxonomic and ecological change across three extinction events of increasing taxonomic magnitude: the early Late Ordovician M4/M5 extinction, the Late Devonian mass extinction (Givetian/Frasnian and Frasnian/Famennian boundaries), and the end-Ordovician mass extinction. Taxonomic and ecological changes during each extinction were contrasted by classifying organisms into genera and ecological lifestyles, followed by analysis with additive diversity partitioning, ordination, and relative abundance distributions.

In terms of additive diversity partitioning, taxonomic extinction is similar for both the Ordovician/Silurian and Late Devonian extinction events, but the Late Devonian shows much greater effects in terms of lifestyles. When controlling for the effects of extinction alone, lifestyle diversity remains high for the Ordovician/Silurian event, but decreases drastically for the Late Devonian extinction. The M4/M5 shows minor extinction for both genera and lifestyles. In terms of ordination, the greatest taxonomic separation was observed across the Ordovician/Silurian boundary while the greatest ecological separation was observed across the Late Devonian boundary. In terms of relative abundance distribution analyses, the total change in relative abundance was similar for the Ordovician/Silurian and Late Devonian extinction in terms of genera and lifestyles. Taken together, this suggests that while many taxa go extinct across the Ordovician/Silurian boundary, post-extinction taxa fill the same ecological roles as pre-extinction taxa. In contrast, post-extinction taxa during the Late Devonian only inhabited a fraction of the ecological roles as pre-extinction taxa. These results underscore that the magnitude of taxonomic change due to extinction can be a poor predictor of the amount of ecological change.

# Oral Session Two B: Ice/Hydrology

Saturday, March 17  
11:00 – 11:45 am, 116 EES

<b>Time</b>	<b>Presenter</b>	<b>Advisor</b>	<b>Title</b>
11:00	Lucas Zoet	Sridhar Anandakrishnan	Discrete Movement of Glaciers
11:15	Ryan Swanson	Kamini Singha	Geoelectrical Evidence of Dual-Domain Mass Transfer
11:30	Katy Gerecht	Kamini Singha	Stream temperature response to storms indicates seasonal groundwater decoupling

# Discrete Movement of Glaciers

**Lucas Zoet**

Ph.D. Student, Post comps

**Advisor: Sridhar Anandakrishnan**

Richard B. Alley, Penn State University

We report on a pattern of repeating earthquakes associated with the flow of David Glacier through the Transantarctic Mountains at its base. The seismic events ( $M_w=1.8$ ) recurred regularly (approximately 20 minutes) for a 275-day span in 2001 and 2002. Before and after this 275-day period, the recurrence was orders of magnitude more infrequent and irregular. The events are likely caused by an asperity (55km from grounding line) beneath David Glacier that regularly releases stress accumulated by the flow of the glacier. We suggest that the change in seismic behavior is due to changes in debris concentration of the basal ice over time. This results in the asperity experiencing changing rheological values over time, resulting in the observed behavior. A secondary effect was found to modulate the spacing between events through the loss and addition of back stress in tidal fluctuations.

In order to study how changes in entrained debris affects deformation of ice we froze a number of ice samples with varying percentages of debris (1-50% by weight). We show that an increase in basal debris concentration can alter the velocity-strengthening/weakening boundary thus having large impacts on the ability of the system to stick slip or slide stably. The stiffness of the shearing apparatus was reduced in order to allow stick-slip behavior to occur, which was successfully produced in the lab. Similarities between laboratory results and field observations are beginning to emerge which will help to scale from the one to the other.

Both the inter-event spacing and the magnitude of the events changes slowly over time, and are related to tidal amplitudes. There is a lag between the tidal amplitude maxima and the inter-event spacing maxima where at high tide the mean inter-event time is longest. It is theorized that the added backpressure causes a decrease in flow velocity resulting in less displacement at the asperity as well as a longer healing period at the ice-rock interface. This increased healing results in a stronger ice-bed interface at the time of slip, which leads to higher magnitude events.

The ability of the system to transition between stick and slip regimes results in periods where a significant part of the stored energy is released quickly, providing a mechanism to fracture the rock at the asperity. Fracturing of the asperity would result in brief periods of increased rates of erosion at the base of glacier. The seismic data from David Glacier show that this increased rate of seismicity only lasts for finite intervals, suggesting that this mechanism is strongly heterogeneous in space and time, but could encompass a significant percentage of the total subglacial erosion.

# Geoelectrical Evidence of Dual-Domain Mass Transfer

**Ryan David Swanson**

Ph.D. Student, Pre-comps

**Advisor: Kamini Singha**

Frederick D. Day-Lewis, USGS

Andrew Binley, Lancaster University

Kristina Keating, Rutgers University, Newark

Roy Haggerty, Oregon State University

Understanding the fate and transport of contaminants in saturated porous media is a complex, poorly understood process. The advection-dispersion model often fails to match contaminant transport data, resulting in more complex models used to describe solute transport. Of particular interest is the dual-domain mass transfer (DDMT) model, which partitions the total porosity into a mobile and immobile domain. The DDMT model allows for a better fit of breakthrough curve data, yet experimental evidence is needed to quantify the amount of immobile and mobile domains and the rate that solutes that exchange between them. Here, we conduct column solute tracer tests and collect nearly co-located bulk electrical conductivity ( $\sigma_b$ ) and fluid conductivity ( $\sigma_f$ ) measurements on unconsolidated, well-sorted sand and the porous zeolite clinoptilolite in order to monitor the exchange of solutes between domains. We use Nuclear Magnetic Resonance (NMR) and other methods to characterize the media and quantify the mobile and immobile domain *a priori*. Our results show extensive tailing behavior in both  $\sigma_f$  and  $\sigma_b$  in the zeolites, providing evidence for a mobile-immobile framework and solute exchange. Transport parameters are estimated by minimizing the transformed RMSE between the observed and simulated  $\sigma_f$  to emphasize the fit to the late-time behavior. These best-fit parameters match our NMR measurements of immobile and mobile pore space and provide the first direct electrical evidence of dual-domain mass transport and solute exchange at the lab scale.

# **Stream temperature response to storms indicates seasonal groundwater decoupling**

**Katy Gerecht**

Ph.D. Student, Pre-comps

**Advisors: Kamini Singha and Mike Gooseff**

Here we investigate the impact of storm events on the temperature regime of a headwater stream located in Huntingdon County in central Pennsylvania. The stream's 1.5 km<sup>2</sup> watershed is more than 90% forested. Stream temperature data collected from April to October of 2011 show that during storm events this rural headwater stream can exhibit a more urban-like stream temperature response. We see sharp increases in stream temperature during storm events of up to 3.8 °C. We hypothesize that these anomalous stream temperature responses are seasonally dependent and point to minimized groundwater buffering of stream temperatures primarily during the spring. A simple 1D heat transport model is used to better understand the physical processes that affect stream temperature during storm events. Future work will include instrumentation of other nearby streams during the 2012 field season and expansion of the model's complexity.

# Oral Session Three: Biogeochemistry

Saturday, March 17  
1:30 – 2:45 pm, 114 EES

<b>Time</b>	<b>Presenter</b>	<b>Advisor</b>	<b>Title</b>
1:30	Ying Cui	Lee Kump	Carbon injection during the end Permian mass extinction: Model inversion of carbon isotope excursion
1:45	Clayton Magill	Kate Freeman	High-resolution reconstruction of early human habitats at FLK <i>Zinjanthropus</i> (Olduvai Gorge) using lipid biomarker and isotope signatures
2:00	Elizabeth Denis	Kate Freeman	A Fiery Investigation of the Paleocene-Eocene Thermal Maximum (PETM) using Polycyclic Aromatic Hydrocarbons (PAHs)
2:15	Laurence Bird	Kate Freeman	Coenzyme F430, quantification and isotope analysis from the Eel River Basin, California

# **Carbon injection during the end Permian mass extinction: Model inversion of carbon isotope excursion**

**Ying Cui**

Ph.D. Student, Pre-comps

**Advisor: Lee Kump**

Andy Ridgwell, School of Geographical Sciences, University of Bristol

Katja Meyer, Department of Geological & Environmental Sciences, Stanford University

Numerous lines of geochemical and stable isotopic evidence indicate that the most devastating mass extinction that occurred at the end of Permian is tied to drastic climate change induced by CO<sub>2</sub> addition. Catastrophic end-Permian Siberian volcanism may have released large amount of CO<sub>2</sub> into the atmosphere and pushed the Earth's system beyond a critical threshold causing the mass extinction. However, the injection rate, total amount and source of CO<sub>2</sub> is largely unknown. We conducted a suite of simulations using carbon isotope records from the Gartnerkofel-1 core in Carnic Alps, Austria, and section D Meishan in Zhejiang province, China. An Earth System Model of Intermediate Complexity (EMIC) (Genie-1; <http://www.genie.ac.uk>) was used to extract the pattern of CO<sub>2</sub> release needed to replicate the observed carbon isotope excursion across the P-T boundary. We also assessed the ocean saturation profile, surface water pHs and the ocean buffering capacity in response to the predicted greenhouse gas addition. As with the Paleocene-Eocene boundary event, end-Permian rates of CO<sub>2</sub> addition are small compared with fossil-fuel burning but protracted. In addition, the lack of pelagic carbonate production and thus a seafloor carbonate buffer made the Earth system much more sensitive to CO<sub>2</sub> addition.

# High-resolution reconstruction of early human habitats at FLK *Zinjanthropus* (Olduvai Gorge) using lipid biomarker and isotope signatures

**Clayton R Magill**

Ph.D. Student, Post comps

**Advisor: Katherine H Freeman**

Gail M Ashley, Department of Earth and Planetary Sciences, Rutgers University

The FLK *Zinjanthropus* (*Zinj*) archaeological site at Olduvai Gorge plays a central role in understanding the origins of early human (hominin) behavior because of its unusual high-density co-occurrence of fossilized bones and stone tools. Many models of hominin behavior utilize environmental contexts, yet reconstructions remain highly controversial for FLK *Zinj* and the surrounding landscape.

We use lipid biomarker and isotope signatures of organic matter in ancient soil (paleosol) sediments to shed light on hominin landscapes at Olduvai Gorge. Sediments recovered from FLK *Zinj* and 18 facies equivalents from the surrounding 2000 m<sup>2</sup> consist of green clays (smectite) deposited during episodic lake-margin flooding about 1.839 million years ago. Carbon-isotope ratios ( $\delta^{13}\text{C}$ ) of bulk organic matter vary from  $-18.6\text{‰}$  to  $-27.1\text{‰}$  while plant biomarker  $\delta^{13}\text{C}$  vary from  $-19.4\text{‰}$  to  $-33.1\text{‰}$ . Stone tools and cut-marked bones show highest concentrations in sediments with negative  $\delta^{13}\text{C}$  and woody plant tissue (lignin) signatures. Samples from a spring (tufa) deposit about 200 m north of FLK *Zinj* show high concentrations of sedge biomarkers.

We interpret our results as evidence for patchy landscapes ranging from closed woodland to wetland. Densest archaeological accumulations occur near FLK *Zinj* and negative  $\delta^{13}\text{C}$  at this site suggest a woodland patch. Nearby tufa deposit and sedge biomarkers suggest the occurrence of perennial freshwater source. These two landscape patches contrast with proxy evidence for extensive grassland occurrence in this basin. We conclude that hominins selected this site for carcass transport and processing because it afforded shelter and potable water in an otherwise harsh environment.

# **A Fiery Investigation of the Paleocene-Eocene Thermal Maximum (PETM) using Polycyclic Aromatic Hydrocarbons (PAHs)**

**Elizabeth Denis**

Pre-comps

**Advisor: Kate Freeman**

**Co-advisor: Lee Kump**

Past hyperthermal events, such as the Paleocene-Eocene Thermal Maximum (PETM), can serve as analogs for current and future climate changes. During the PETM (~55.9 Ma) a significant amount of CO<sub>2</sub> was released in ~10-20 ky from an unknown reservoir and global temperatures increased by ~5°C over a span of ~170 ky. This event coincided with a global negative carbon isotope excursion, suggesting a massive perturbation to the global carbon cycle and a large release of <sup>13</sup>C-depleted carbon to the atmosphere, oceans and biosphere. Several proposed sources of this carbon include ocean-floor clathrates, thermogenic methane, and burning of peat and/or shallowly buried coal, but the exact source(s) remain unknown. The Paleocene was a time of extensive terrestrial organic carbon burial and some authors have suggested that a change in climate induced burning of the <sup>13</sup>C-depleted carbon deposits. Understanding the source and amount of carbon released during the PETM provides constraints on climate sensitivity to CO<sub>2</sub>, which is critical for evaluating the response of the Earth system to current anthropogenic changes to the carbon cycle.

In this study, polycyclic aromatic hydrocarbons (PAHs), organic compounds produced as aerosols during combustion, are used as fire markers to investigate the occurrence of fire during the PETM from outcrop and long core samples from the Bighorn Basin, WY. I hypothesize that climate-induced burning will be evident in these Paleocene-Eocene sediments as indicated by an increase in PAHs during the PETM. The Bighorn Basin preserves one of the most complete terrestrial records of the PETM in the world and encapsulates upper Paleocene to lower Eocene rocks for both pre- and post- PETM analyses. Preliminary results of several core samples analyzed using gas chromatography-mass spectrometry (GC-MS) in selective ion monitoring (SIM) mode confirm the presence of PAHs with abundances of various PAHs on the order of 0.1 – 100 ng/g dry sediment. By comparing the relative abundance of PAHs from the late Paleocene through the early Eocene, temporal variations in fire occurrence will be evaluated. This study will provide a fire record for the late Paleocene and early Eocene and provide insights into fire and climate feedbacks during a warm, CO<sub>2</sub>-rich climate.

# Coenzyme F430, quantification and isotope analysis from the Eel River Basin, California

**Laurence Bird**

Ph.D. Student, Pre-comps

**Advisor: Kate Freeman**

Jamey Fulton, Woods Hole Oceanographic Institution

Victoria Orphan, California Institute of Technology

Large amounts of methane are oxidized to carbon dioxide by communities of methanotrophic archaea and sulphate reducing bacteria, preventing this greenhouse gas from reaching the atmosphere [1,2]. Methyl-coenzyme M reductase, an enzyme traditionally associated with methanogenesis, has recently been linked to the anaerobic oxidation of methane [2]. Cofactor F430 is a tetrapyrrole nickel complex contained within the active site of methyl-coenzyme M and appears to be used in both methanogenesis and methanotrophy [2,3]. Here we provide evidence for F430 in a sediment core from the Eel River Basin (California) and pure cultures of *Methanosarcina acetivorans*. The identification of F430 in environmental samples is particularly important as it provides evidence for anaerobic methane oxidation in a low oxygen environment via the reversal of the enzymes involved in methanogenesis.

Using a new approach F430 can be quantified from natural samples and isolated in a pure enough state for stable isotopic analysis ( $^{15}\text{N}$  and  $^{13}\text{C}$ ). F430 is isolated using multi-dimensional preparatory and high-performance chromatographic separations. Compound identity and purity are confirmed using molar C:N ratios, UV absorbance and  $\text{MS}^n$  detection and fragmentation. Quantification is performed using a Diode array detector and isotope analysis using a nano EA-IRMS. Our results provide valuable insight into the biochemistry of life in anaerobic environments and the methane cycle.

[1]Orphan (2001) *Science* 293 5529 484 [2]Scheller (2010) *Nature* 465 7298 606 [3]Mayr (2008) *Journal Of The American Chemical Society* 130 32 10758

# Oral Session Four A: Astrobiology

Saturday, March 17  
3:00 – 4:00 pm, 114 EES

<b>Time</b>	<b>Presenter</b>	<b>Advisor</b>	<b>Title</b>
3:00	Becky McCauley	Jennifer Macalady	Carbon Fixation Pathways in Energy-Limited Microbial Communities in the Anoxic Subsurface (Frasassi Caves, Italy)
3:15	Jamie Brainard	Hiroshi Ohmoto	Volcanogenic massive sulfide deposits host the evidence for sulfate-rich Archean oceans
3:30	Karen Smith	Christopher House	Metabolic Precursors in Carbonaceous Chondrites
3:45	Kyle Rybacki	Lee Kump	Hyperventilation during the Paleoproterozoic Great Oxidation Event

# Carbon Fixation Pathways in Energy-Limited Microbial Communities in the Anoxic Subsurface (Frasassi Caves, Italy)

**Becky McCauley**

Ph.D. Student, Pre-comps

**Advisor: Dr. Jennifer Macalady**

D. S. Jones, Penn State

I. Schaperdoth, Penn State

J. L. Macalady, Penn State

A biofilm with rope-like morphology was recovered by divers from the anoxic and sulfidic water of a remote cave lake (Lago Infinito). The biofilm has high species richness, and is dominated by bacteria in the phyla *Deltaproteobacteria* and *Chloroflexi*. *Deltaproteobacteria* in sulfate-reducing clades make up a significant fraction of the community, consistent with geochemical data and thermodynamic calculations showing that sulfate reduction is the most energetically favorable metabolism. *Chloroflexi* in organoheterotrophic clades make up approximately 10% of the population. In addition to dissolved organic carbon (5  $\mu\text{M}$  as acetate; >1ppm C) and sulfide (175  $\mu\text{M}$ ), ammonium (100  $\mu\text{M}$ ), and  $\text{H}_2$  are plausible electron donors. However, electron acceptors other than sulfate (1.6 mM) are non-detectable ( $\text{NO}_3^-$ ,  $\text{NO}_2^-$ ,  $\text{Fe}^{3+}$ ,  $\text{Mn}^{4+}$ ). Roughly 1/3 of the 16S rRNA fragments retrieved from the biofilm have no cultivated relatives at the order or phylum level.

In this energy-limited environment (i.e. no light or oxygen) with low levels of dissolved organic carbon, we investigated carbon fixation based on metagenomic sequences and carbon isotopic signatures. I analyzed metagenomic reads for similarity to known carbon fixation enzymes of the known carbon fixation pathways. Additionally,  $\delta^{13}\text{C}$  for biofilm organic carbon and dissolved inorganic carbon were compared. The data suggest that genes for several carbon fixation pathways are present representing a diverse phylogenetic clades in the microbial community, but the Calvin Cycle may dominate due to the carbon isotope fractionation values.

# Volcanogenic massive sulfide deposits host the evidence for sulfate-rich Archean oceans

**Jamie L. Brainard**

Ph.D. Student, Pre-comps

**Advisor: Hiroshi Ohmoto**

Andrew Chorney, Penn State

Recent researchers have suggested that the Archean oceans were sulfate poor ( $<0.1$  mM  $\text{SO}_4^{2-}$ , compared to 28 mM today), because the atmosphere was supposedly poor in  $\text{O}_2$  ( $p\text{O}_2 < 10^{-6}$  atm) to completely oxidize the sulfur-bearing volcanic gases ( $\text{H}_2\text{S}$  and  $\text{SO}_2$ ) and sulfide minerals in soils to  $\text{SO}_4^{2-}$ . However, such a scenario cannot explain the abundance of pyrite of Archean ages, much like those of younger ages, because these pyrites most likely formed by bacterial (or thermochemical) reduction of seawater  $\text{SO}_4^{2-}$ .

One of the strongest lines of evidence for  $\text{SO}_4^{2-}$  rich Archean oceans comes from volcanogenic massive sulfide (VMS) deposits and their host rocks. VMS deposits, such as the black smoker deposits on MORs, formed on and beneath the seafloor by reactions between submarine hydrothermal fluids (typically  $\sim 50^\circ$  to  $\sim 450^\circ\text{C}$ ) and the local seawater. The hydrothermal fluids evolved mostly through reactions between hot rocks and deep-circulating seawater, rather than derived directly from magmas. Therefore, the mineralogy and geochemistry of VMS deposits and their alteration zones reflect the chemistry of the contemporaneous ocean water. Phanerozoic VMS deposits are characterized by the abundance of sulfate minerals (barite and anhydrite) and pyrite, and their alteration zones by increased  $\text{Fe}^{3+}/\text{Fe}^{2+}$  ratios due to the involvement sulfate-rich seawater: some of the  $\text{H}_2\text{S}$  used to form the pyrite was generated by reduction of seawater sulfate by FeO components in rocks, resulting in the increases of  $\text{Fe}^{3+}/\text{Fe}^{2+}$  ratios. The  $\sim 3.2$  Ga Panorama Formation of Western Australia hosts many VMS deposits with mineralogy, geochemistry, and associated alteration zones are essentially identical to those of Phanerozoic ages, suggesting that the processes of submarine mineralization and the sulfate content of the seawater at 3.2 Ga were essentially the same as today.

Many other Archean VMS deposits and their alteration zones host barite, such as the  $\sim 3.46$  Ga Big Stubby deposits, the 3.26 Ga Fig Tree deposit, the 2.6 Ga Geco deposit, and the 2.7 Ga Hemlo deposits, suggesting that the Archean oceans remained sulfate-rich. The only major difference between the sulfate in the Archean oceans and that in the Phanerozoic oceans was the  $\delta^{34}\text{S}$  values, between +2 and +5‰ during the Archean, but between +10 and +35‰ for the Phanerozoic. This raises the question whether the isotopic evolution of the seawater sulfate through geologic history was due to changes in: (1) the metabolism of sulfate-reducing bacteria, reflecting (an) environmental change(s) (e.g., ocean temperature), and/or (2) in the fluxes of  $\text{SO}_4^{2-}$  to/from the oceans.

# Metabolic Precursors in Carbonaceous Chondrites

**Karen E. Smith**

Ph.D. Student, Post comps

**Advisor: Christopher H. House**

Michael P. Callahan, NASA Goddard Space Flight Center

Aaron S. Burton, NASA Goddard Space Flight Center/ORAU

Jason P. Dworkin, NASA Goddard Space Flight Center

Nicotinic acid (also known as niacin or vitamin B<sub>3</sub>), a pyridine carboxylic acid, is a precursor to nicotinamide adenine dinucleotide (NAD<sup>+</sup>), which is essential to all of life because it plays a vital role in metabolism. Sources of pyridine carboxylic acids may have included both abiotic synthesis on the primitive Earth (Cleaves and Miller, 2001) and exogenous delivery by meteorites (Pizzarello *et al.*, 2001). We have developed a liquid chromatography-high resolution Orbitrap mass spectrometry method for the detection of nicotinamide, three pyridine carboxylic acids, and five pyridine dicarboxylic acids in carbonaceous chondrite meteorites. We measured parts-per-billion abundances of pyridine carboxylic acids and find that they correlate with the aqueous alteration of the asteroid parent body. We will present our latest results of pyridine carboxylic acids in eight CM2 carbonaceous chondrites and discuss possible formation pathways and their relevance to astrobiology.

Cleaves, H. J., and Miller, S. L. (2001) The Nicotinamide Biosynthetic Pathway Is a By-Product of the RNA World. *Journal of Molecular Evolution*, 52: 73-77.

Pizzarello, S., Huang, Y., Becker, L., Poreda, R. J., Nieman, R.A., Cooper, G., and Williams, M. (2001) The Organic Content of the Tagish Lake Meteorite. *Science*, 293: 2236-2239.

# Hyperventilation during the Paleoproterozoic Great Oxidation Event

**Kyle S. Rybacki**

Ph.D. Student, Pre-comps

**Advisor: Dr. Lee Kump**

One of the most important events in Earth history was the establishment of an oxygen-rich atmosphere. Today, it is widely accepted that the oxygenation of the Earth's atmosphere occurred at ca. 2.45 billion years ago (Ga) based upon the suppression of the mass-independent fractionation of sulfur within the geologic record. Our research proposes to investigate the notion that the 2.0 Ga Shunga-Francevillian negative carbon isotope excursion occurred as the result of a buildup of oxygen in the atmosphere during the preceding positive Lomagundi-Jatuli carbon isotope excursion at ca. 2.2 Ga. Specifically, we intend to test the hypothesis that atmospheric oxygen levels built up to levels that may have exceeded modern during the Lomagundi-Jatuli positive carbon isotope excursion, leading to the subsequent deep oxidative weathering of the continental crust.

Evidence in support of this hypothesis is observed within the subaerial, mafic to intermediate volcanics observed across the Kola Peninsula of Fennoscandia, arctic Russia. These volcanics are characterized by noticeably elevated ferric-ferrous ratios when compared the adjacent volcanic formations. In particular, the ca. 2.06 Ga Kuetsjärvi Volcanic Formation (KVF) is anomalously oxidized with the ratio of oxidized iron to total iron ( $\text{Fe}^{3+}/\Sigma\text{Fe}$ ) varying between 0.30 and 0.95 for the majority of samples. Adjacent volcanic formations have maximum  $\text{Fe}^{3+}/\Sigma\text{Fe}$  primarily less than 0.30. The difference in the oxidation state of iron may partly be explained by the geotectonic environment during eruption, as the two youngest volcanic formations are submarine while the two oldest ones are subaerial. However, the difference in the present redox state of the two subaerial volcanic units is striking and needs to be explained.

Based on the petrographical and geochemical data, it is evident that the high  $\text{Fe}^{3+}/\Sigma\text{Fe}$  ratios are due to post-crystallization oxidation coupled to hematitization and magnetite formation. Petrographic features suggest that this overprinting affected the rocks prior to regional metamorphism, which took place at ca. 1.80 Ga during the Svecofennian orogeny. Oxidation is believed to have occurred during, or immediately following, eruption as evidenced by the incorporation of the oxidized Kuetsjärvi volcanic clasts into the overlying conglomerate unit which does not exhibit pervasive oxidation.

We propose to collect major, trace, and stable isotope geochemical data to construct alteration profiles through individual subaerial lava flows, which will allow us determine the magnitude and characteristics of weathering processes during the Paleoproterozoic in Fennoscandia. Secondary minerals observed within amygdales will also be analyzed geochemically to determine the chemistry of the fluids with which these rocks have interacted. To constrain the timing of hematization and fluid migration through the KVF Formation we propose to date the secondary hematite using the U-Th-He system.

# Oral Session Four B: Sedimentology and Stratigraphy

Saturday, March 17  
3:00 – 4:00 pm, 116 EES

<b>Time</b>	<b>Presenter</b>	<b>Advisor</b>	<b>Title</b>
3:00	Craig Millard	Liz Hajek	What can splay and other overbank deposits tell us about avulsion processes and sedimentation in fluvial systems?
3:15	Daniel Kohl	Rudy Slingerland	Sequence Stratigraphy and Depositional Environments of the Shamokin (Union Springs) Mbr., Marcellus Fm. and Associated Strata in the Middle Appalachian Basin
3:30	Ellen Chamberlain	Liz Hajek	Evaluating avulsion and basin-filling patterns in the Holocene and in ancient fluvial systems
3:45	Nicole West	Eric Kirby	Quantifying Regolith transport at the Susquehanna Shale Hills Critical Zone Observatory, PA, using meteoric $^{10}\text{Be}$

# What can splay and other overbank deposits tell us about avulsion processes and sedimentation in fluvial systems?

**Craig L. Millard**

M.S. Student--Petroleum related

**Advisor: Elizabeth A. Hajek**

Douglas Edmonds, Boston College

Preston Smith, Boston College

Crevasse splays and related facies are common in some avulsive fluvial systems, while being nearly absent in others. As such, the study of splay and other overbank deposits may be fundamental to understanding the processes of fluvial avulsion and basin filling in terrestrial systems. Progradational avulsive systems such as the modern Saskatchewan River (Saskatchewan, Canada) and the Paleocene-Eocene Willwood Formation (Big Horn Basin, Wyoming) contain extensive heterolithic avulsion deposits consisting of inter-bedded fines (clay and fine silt) and coarser sediments (coarse silt and sand) generally interpreted as overbank sediments—including splays—deposited during the avulsion sequence and prior to full establishment of the main channel. Conversely, incisional avulsive systems such as the modern Klip River (eastern South Africa) and tributaries of the Murray River (Victoria, Australia) contain few—if any—splay deposits despite undergoing identified avulsion events.

Field observations from the Paleocene Fort Union (Bighorn Basin, Wyoming) and Willwood Formations documented extensive splay deposits lateral to and beneath channel deposits traceable for hundreds of meters and extensively mottled paleosol horizons laterally traceable for many kilometers. In the Late Cretaceous-Paleocene Ferris Formation (Hanna Basin, Wyoming), lateral splays are very rare and where present are vertically thin and taper out within approximately 10 meters. Floodplain deposits consist of very-fine grained carbonaceous material typical of water-logged conditions, and channel bodies are incised directly into these previously distal floodplain deposits with no presence of heterolithic avulsion deposits.

Splay development and frequency in the Murray, Sandover-Bundey (Northern Territory, Australia), Saskatchewan, and Upper Columbia (British Columbia, Canada) River systems was determined using aerial photography from *Google Earth*. Within these systems, the splays differ in appearance, sediment transport characteristics, and mass-balance distribution. Based on preliminary analysis, the primary controls on splay development and abundance appear to be the type of water routing on the floodplain (diffusive vs. advective) and the grain-size distribution of sediments within the channel.

# **Sequence Stratigraphy and Depositional Environments of the Shamokin (Union Springs) Mbr., Marcellus Fm. and Associated Strata in the Middle Appalachian Basin**

**Daniel Kohl**

M.S. Student, Petroleum related

**Advisor: Dr. Rudy Slingerland**

Dr. Mike Arthur, Dr. Terry Engelder, The Pennsylvania State University

This study uses approximately 1000 wireline well logs, 8 cores, and 23 outcrops in the northern Appalachian basin (PA, NY, OH, WV, MA) to construct a sequence stratigraphic framework and depositional model of the lower portion (Union Springs mbr.) of the Middle Devonian Marcellus Formation and associated strata. Chronostratigraphic surfaces defined using sequence stratigraphic principles demonstrate that prior to Union Springs time, carbonate deposition in the western and northwestern portions of the basin resulted in a thick carbonate bank (Onondaga Fm.) with greater than 220 ft (61 m) of relief relative to the central, deeper portions of the basin. Continued base level rise during late Onondaga to early Union Springs time drowned out this carbonate bank and produced a relatively deep, stratified basin into which the lower portion of the Marcellus Fm was deposited. Correlations in the Marcellus Fm. indicate the Marcellus was deposited as a series of prograding muddy clinofolds associated with the Mahantango delta complex. Base level fall within the Union Springs Fm. resulted in a forced regression and progradation of clastics from the east. An onset of base-level rise following the upper Union Springs mbr./ lower Mahantango Fm. forced regression, sequestered clastic material to the east enabling widespread limestone (Purcell Mbr.) deposition on the bathymetric highs of the basin. Thickest, high TOC Union Springs mbr. occurs in a NE to SW belt across west-central Pennsylvania which is associated with the greatest paleo-water depth (a minimum of 450ft , 137m) and was furthest from sources of dilution in the west and east.

# Evaluating avulsion and basin-filling patterns in the Holocene and in ancient fluvial systems

**Ellen Chamberlin**

Ph.D. Student, Pre-comps

**Advisor: Liz Hajek**

Internal (autogenic) processes, primarily channel avulsions, are important in building stratigraphy in alluvial basins, and can add significant noise to stratigraphic interpretations of external conditions like climate and tectonics. Field, experimental and numerical studies have identified autogenic stratigraphy produced at long timescales, including those usually associated with external controls; even on  $10^5$  or  $10^6$  -year timescales, avulsion processes control how and where basins fill because they are an essential mechanism for flow and sediment routing. Here we present preliminary tests on the limits of statistical measures that quantify autogenic stratigraphy, and propose field research to analyze the role mud content on avulsion stratigraphy.

The compensation and the clustering indexes are statistical measures that quantify the evenness or randomness of sedimentary basin filling. When avulsions preferentially divert flow and sediment to regional topographic lows, basins fill evenly (or compensationally), producing stratigraphy with evenly spaced channel bodies. In this study, we analyzed Holocene stratigraphy of the Rhine-Meuse delta in the Netherlands to test the temporal and spatial limits of the compensation index. With 10 meters of sediment accumulation (deposited over 9000 years), and the compensation statistic shows uncorrelated, random deposition ( $k = 0.538$ ), even though the Rhine avulsion pathways were likely compensational. These results may indicate that the Rhine-Meuse system is below the threshold of statistical detection. This suggests that we cannot assess basin-filling patterns without looking at the ancient record.

The Cretaceous Williams Fork Formation in western Colorado is an ideal place to analyze autogenic basin filling, because it is a thick fluvial formation with well-preserved, well-exposed avulsion deposits. Williams Fork stratigraphy will be used to determine which internal factors are most important in building compensational or clustered autogenic stratigraphy. Because cohesive muds promote channelized floodplains that corral and steer flow, we hypothesize that muddy systems will generate more organized, clustered stratigraphy, whereas less cohesive, sandy systems will generate more compensational or uncorrelated stratigraphy. The Williams Fork Formation will be used to test this hypothesis because it has a contrasting lower mud-rich member, and an upper sand-rich member.

# Quantifying Regolith transport at the Susquehanna Shale Hills Critical Zone Observatory, PA, using meteoric $^{10}\text{Be}$

**Nicole West**

Ph.D. Student, Post Comps

**Advisor: Eric Kirby**

Meteoritic  $^{10}\text{Be}$  data from 88 samples of bulk regolith collected along north and south hillslopes at the Susquehanna Shale Hills Critical Zone Observatory (SSHO) provide first-order constraints on the timescales of regolith formation. The SSHO is located in the presently temperate climate zone of central Pennsylvania; however, sustained periglacial climate during the time of maximal extent of the Laurentide ice sheet (~19-21 ka) and deforestation during mid-19th Century charcoal production may have exerted significant influence on regolith production. Here, we quantify soil residence times and corresponding rates of regolith production and transport at SSHO, using meteoric  $^{10}\text{Be}$  in samples of regolith collected at 25 locations along each hillslope from ridge top to valley floor. Hillslopes within the SSHO are relatively planar, but exhibit a pronounced asymmetry; southern slopes are steeper (~20°) than northern slopes (~15°). Meteoric  $^{10}\text{Be}$  inventories are similar at the north and south ridgetop sites ( $1.89 \pm 0.55$  at/cm<sup>2</sup> and  $1.63 \pm 0.41$  at/cm<sup>2</sup>, respectively) and generally increase with position downslope. Assuming that the delivery of meteoric  $^{10}\text{Be}$  to regolith is balanced by its removal via erosion, the total meteoric  $^{10}\text{Be}$  inventories at the north and south ridgetops are consistent with soil  $^{10}\text{Be}$  residence times of  $10.5 \pm 3$  ky and  $9.1 \pm 2$  ky, and steady lowering rates of  $16 \pm 3.9$  m/My and  $19 \pm 4.9$  m/My, respectively. Similarly, regolith transport rates are consistent between the two hillslopes, with flux rates increasing downslope from 5.1 cm<sup>2</sup>/y to 12.1 cm<sup>2</sup>/y on the southern hillslope and from 6.2 cm<sup>2</sup>/y to 18.9 cm<sup>2</sup>/y on the northern hillslope.

Comparison of our results with previously-published estimates of regolith production rates inferred from U-series disequilibrium reveals that estimates of downslope regolith flux calculated using meteoric  $^{10}\text{Be}$  are on the same order as production. Although rates of regolith production and downslope flux are similar, their differences suggest a subtle thickening of regolith as production slightly outpaces downslope transport. Overall, the meteoric  $^{10}\text{Be}$  results suggest that most of the regolith on hillslopes within the SSHO watershed formed during the Holocene since the time of periglacial influence.

## **Please give us your feedback!**

The committee was particularly excited about having the colloquium over a weekend so more people could participate. Please tell us what you thought so we can make it even better next year.

You can remove this page and place it in the comments box at the door of 114 EES or give it to one of the committee members. You can also email Lauren Milideo or Jamie Brainard at [lem231@psu.edu](mailto:lem231@psu.edu) or [jlb5156@psu.edu](mailto:jlb5156@psu.edu).